

Rigorous Bounds on Massive Lepton Pair Production
and Tests of Parton Models

MARTIN B. EINHORN and ROBERT SAVIT
National Accelerator Laboratory, Batavia, Illinois 60510

ABSTRACT

Using Lagrange inequality multipliers, we derive rigorous upper bounds on cross sections for the process $pN \rightarrow \ell^+ \ell^- + X$, in the context of the parton model. For definiteness, we work with a colored quark version of the parton model, but our results are easily generalizable to other versions. The constraints we impose are given by our knowledge of νW_2 for protons and neutrons. Then, in a separate problem we add further constraints derived from considerations of the recent neutrino and antineutrino data from Gargamelle. Our upper bounds fall below the Brookhaven data. We conclude, therefore, that at least one of the following statements is true:

- 1) The experimentally observed cross section is not the scaling limit for the process.
- 2) The Drell-Yan formula for $pN \rightarrow \ell^+ \ell^- + X$ must be modified.
- 3) The colored-quark parton model is wrong.



I. INTRODUCTION

During the last few years, parton models for weak electromagnetic and even for strong interactions have received widespread attention.^{1, 2} Unfortunately, the model has not been formulated in a mathematically precise and physically consistent way, and consequently, it is obscure just what the "parton model" really is. However, certain general features are common to nearly all discussions; for example, that the partons are constituents of hadrons having a point-like coupling to the photon.³ From these general features follow the most straightforward consequences of the model: the general forms for the lepton production structure functions, and certain sum rules and inequalities which follow from the general form.⁴ On the other hand, the least believable consequences are those predictions which depend on very specific assumptions concerning the forms of the probability distributions for each parton.⁵ The introduction of such assumptions has usually been motivated by a desire to get some handle on the implications of the parton model for various experimental processes.⁶ However, another approach is possible which may be more meaningful. Regarding some data as constraints among the parton distribution functions, one often may obtain rigorous upper or lower bounds for other cross sections. Aside from its intrinsic theoretical interest, such inequalities, when applied to processes not yet measured may be useful to experimentalists designing new experiments. Once

the data have been collected, the bounds provide rigorous tests of whether the data are compatible with the general, underlying features of the model.

In this paper, we utilize a general mathematical technique for obtaining such bounds. The method involves the introduction of Lagrange multipliers for both equality and inequality constraints. Inasmuch as a pedagogical presentation of the mathematical theory has already been given,⁷ we restrict ourselves in this paper to illustrating the method for the process of heavy lepton pairs produced in hadronic collisions. It will be apparent, however, that our method is applicable to a wide range of physical phenomena.

In parton models, as shown by Drell and Yan,⁸ the cross section in the deep inelastic limit for production of a heavy lepton pair in proton-proton collisions is given by

$$\begin{aligned} Q^4 \frac{d\sigma}{dQ^2} &= \frac{4}{3} \pi \alpha^2 \tau \int_{\tau}^1 \frac{dx}{x} \sum_i e_i^2 [q_i(x) \bar{q}_i(\tau/x) + \bar{q}_i(x) q_i(\tau/x)] \\ &= \frac{8}{3} \pi \alpha^2 \tau \int_{\tau}^1 \frac{dx}{x} \sum_i e_i^2 q_i(x) \bar{q}_i(\tau/x) \quad (1) \end{aligned}$$

where $\tau \equiv Q^2/s$, e_i = charge of parton of type i ,

x = longitudinal fraction of proton's momentum carried by parton,

and $q_i(x)$ = probability of finding a parton of type i at x in a proton.

The derivation of this formula seems to neglect strong interactions

(such as w_{ee} parton exchanges) between the protons. Whether such effects modify the cross section is an open question.⁹ We will return to discuss this point later, however, it is certainly in the spirit of the parton model that interactions among wees do not alter the form of the hard parton distributions. Consequently, the effects of the strong interactions might be essentially to multiply the entire right hand side by some overall normalization constant, without altering the shape of the cross section. These questions will be discussed in more detail elsewhere.

In the following, we shall derive upper bounds on this cross section under a variety of constraints on the parton distributions which arise from data on the related cross sections for deep inelastic leptonproduction. The outline of the paper is as follows: In the next section, we present the solution of a mathematical problem which contains the essential features of the physical problem. In Sec. III, we derive an upper bound on $pp \rightarrow \mu^+ \mu^- X$ and on $pn \rightarrow \mu^+ \mu^- X$ based on the electroproduction data from SLAC. In Sec. IV, we discuss further constraints imposed by neutrino cross sections. This section is subdivided into a phenomenological discussion of existing neutrino data (and what we can expect in the next few years) followed by the mathematical solution of the problem posed. Finally, we conclude in Sec. V with a discussion of the implications of our results and suggestions for future work.

The sequence of figures is fairly self-explanatory without reference to the text. Readers interested only in our results and not how they are

derived, are advised to simply read the figure captions and concluding remarks in Sec. V.

II. PROTOTYPICAL PROBLEM

We begin the discussion with a mathematical prototype of the problems which will concern us later:

Maximize the functional

$$J = \int_{\tau}^1 \frac{dx}{x} [p(x)\bar{p}(\tau/x) + \bar{p}(x)p(\tau/x)] \quad (2)$$

subject to the following constraints on the functions p and \bar{p} :

$$p(x) + \bar{p}(x) = P(x) \quad [P(x) \text{ a given function } \geq 0]$$

$$p(x) \geq 0, \quad \bar{p}(x) \geq 0.$$

Although not really necessary, for pedagogical purposes we will solve this problem by the method of Lagrange multipliers. Since we wish to emphasize the role of the positivity constraints, we use the equality constraint to eliminate one of the variables, say, $\bar{p}(x)$. So our problem is to maximize

$$J = \int_{\tau}^1 \frac{dx}{x} \left\{ p(x) [P(\tau/x) - p(\tau/x)] + [P(x) - p(x)] p(\tau/x) \right\} \quad (3)$$

subject to $0 \leq p(x) \leq P(x)$.

These inequalities can be combined in the requirement $p(x)[P(x) - p(x)] \geq 0$.

Introducing the inequality multiplier $\lambda(x) \geq 0$, we consider the auxiliary functional

$$\mathcal{L} = J + 2 \int_{\tau}^1 \frac{dx}{x} \lambda(x) p(x) [P(x) - p(x)] \quad (4)$$

The variational derivative is

$$\frac{\delta \mathcal{L}}{\delta p(x)} = \frac{2}{x} \left\{ P(\tau/x) - 2p(\tau/x) + \lambda(x) [P(x) - 2p(x)] \right\} = 0. \quad (5)$$

To discuss this equation, it is convenient to classify points in pairs $(x, \tau/x)$.

B_{00} : $p(x) = 0,$	$p(\tau/x) = 0$
B_{01} : $p(x) = 0,$	$p(\tau/x) = P(\tau/x).$
B_{10} : $p(x) = P(x),$	$p(\tau/x) = 0.$
B_{11} : $p(x) = P(x)$	$p(\tau/x) = P(\tau/x).$
I: $0 < p(x) < P(x),$	$0 < p(\tau/x) < P(\tau/x).$

The case when $x \in I$, but τ/x is in one of the other sets can be easily ruled out by setting $\lambda(x) = 0$ in Eq. (5).

In B_{00} and B_{11} , it is easy to show that $\lambda(x)P(x) = -P(\tau/x)$ and hence, incompatible with the requirement $\lambda(x) \geq 0$. In B_{01} and B_{10} we find

$$\lambda(x) P(x) = + P(\tau/x),$$

so these critical points are candidates for local maxima. In either case, the contribution to J is the same:

$$\frac{dx}{x} P(\tau/x) P(x)$$

Finally, consider the set I. Here, we are instructed to set

$$\lambda(x) = 0 \quad \text{and} \quad \lambda(\tau/x) = 0, \quad \text{so}$$

$$p(x) = \frac{1}{2} P(x) \quad \text{and} \quad p(\tau/x) = \frac{1}{2} P(\tau/x).$$

Hence, the value of the integrand in this case is smaller than in B_{01} and B_{10} , namely

$$\frac{1}{2} \frac{dx}{x} P(\tau/x) P(x).$$

Actually, the set I can be excluded without evaluating the integrand, because, by considering the second differential, it can be shown to be a saddle point. To demonstrate this, however, requires consideration of the tangent cone, which will be unfamiliar to most readers and, since it is unnecessary here, it has been relegated to Appendix A.

In the problems of physical interest considered below, $p(x)$ and $\bar{p}(x)$ correspond to quark and antiquark distributions. As in the example above, there will be a degeneracy of the maximum value at each point x (B_{01} or B_{10}). Hence there are an infinity of functions p , all leading to the same maximum value for J .

An important point for subsequent applications has to do with another type of constraint in the form of a sum rule

$$N_{\tau} = \int_{\tau}^1 dx [p(x) - \bar{p}(x)] \quad (6)$$

(For $\tau = 0$, this has the standard form of a quantum number constraint.)

Given a value for the left hand side of (6), one can incorporate the constraint in a straightforward way. Since the mathematics is somewhat more involved, and since the determination of the values of N_τ requires further assumptions than the general framework of the parton model, we shall not include such constraints. For many purposes, the omission of the constraints is inconsequential, since, because of the infinite degeneracy referred to above, a wide range of values of N_τ can be accommodated without changing the value of the bound for J.

III. ELECTROPRODUCTION BOUND

We will now take up a problem of direct physical interest. For definiteness, and because it is physically interesting, we shall derive our results for the colored quark version of the parton model. Later we shall comment on the extension of our results to other versions of the parton model. In the uncolored quark model, the structure functions for deep inelastic electroproduction from a proton or neutron are given by¹

$$\left. \begin{aligned} f_2^{\nu p}(x) &= \frac{4}{9} U(x) + \frac{1}{9} D(x) + \frac{1}{9} S(x) \\ f_2^{\nu n}(x) &= \frac{4}{9} D(x) + \frac{1}{9} U(x) + \frac{1}{9} S(x) \end{aligned} \right\} \quad (7)$$

where

$$\left. \begin{aligned} U(x) &= u(x) + \bar{u}(x) \\ D(x) &= d(x) + \bar{d}(x) \\ S(x) &= s(x) + \bar{s}(x) \end{aligned} \right\} \quad (8)$$

Here, u , d , and s are the usual triplet quark distributions. In the colored quark model, they are three times the distribution function for each color. There is excellent data¹⁰ available from SLAC for these distributions for a wide range of x ($0.04 \leq x \leq 1$). The question arises: with no further assumptions, what is the maximum rate for $pp \rightarrow \mu^+ \mu^- X$ given this data? [Recall Eq. (1).]

Although the SLAC data provides only two constraints, it is illuminating to solve the problem in 2 stages. First, we will imagine that someone has presented us with the three functions $U(x)$, $D(x)$, and $S(x)$. (See, in particular, Sec. IV.) We shall find the maximum given these three constraints. Then we shall find the largest value possible subject only to the two constraints provided by the electroproduction data by varying the maximum derived for three constraints.

To be explicit, we want to maximize (for colored quarks)

$$\begin{aligned}
 Q^4 \frac{d\sigma}{dQ^2} = & \frac{4}{9} \pi \alpha^2 \tau \int_{\tau}^1 \frac{dx}{x} \left\{ \frac{4}{9} \left[u(x) \bar{u}(\tau/x) + u(\tau/x) \bar{u}(x) \right] \right. \\
 & + \frac{1}{9} \left[d(x) \bar{d}(\tau/x) + d(\tau/x) \bar{d}(x) \right] \\
 & \left. + \frac{1}{9} \left[s(x) \bar{s}(\tau/x) + s(\tau/x) \bar{s}(x) \right] \right\} \quad (9)
 \end{aligned}$$

given the three functions in Eq. (8). (Actually, our bounds will give us more information: since the integrand of (9) is proportional to the doubly differential cross section, we will also have bounds on this quantity.

See below.) This problem is clearly the direct sum of three problems precisely of the type considered in the preceding section. The maximum is therefore given by

$$Q^4 \frac{d\sigma}{dQ^2} = \frac{4}{9} \pi \alpha^2 \tau \int_{\tau}^1 \frac{dx}{x} \left[\frac{4}{9} U(x) U(\tau/x) + \frac{1}{9} D(x) D(\tau/x) + \frac{1}{9} S(x) S(\tau/x) \right] \quad (10)$$

Before proceeding, it is interesting to pause at this point to inquire how large the bound would be in a model in which there were no strange quarks, $S(x) = 0$. Then, in terms of the electroproduction structure functions, we have

$$U = \frac{3}{5} (4f_{\frac{1}{2}}^{\gamma p} - f_{\frac{1}{2}}^{\gamma n}) \quad (11)$$

$$D = \frac{3}{5} (4f_{\frac{1}{2}}^{\gamma n} - f_{\frac{1}{2}}^{\gamma p})$$

so the bound can be evaluated from the data. [For uncolored quarks, the bound would be three times as large as the value given in Eq. (10).] We present this bound as the dashed line in Fig. 1. (Comparisons with data will be discussed presently.)

In general, of course, we cannot neglect strange quarks, so we regard U , D , and S as variables and maximize Eq. (10) subject to the two constraints, Eq. (7), as well as the positivity requirements, $U \geq 0$, $D \geq 0$, $S \geq 0$. We could solve this problem by considering U , D , and S as independent variables, but it is easier to solve for the two variables U and D , in terms of S .

$$U = \frac{3}{5} [4f \frac{Y^P}{2} - f \frac{Y^n}{2}] - \frac{1}{5} S(x) \tag{12}$$

$$D = \frac{3}{5} [4f \frac{Y^n}{2} - f \frac{Y^P}{2}] - \frac{1}{5} S(x)$$

The positivity requirements then become simply

$$0 \leq S(x) \leq \text{Min} \left\{ 3 [4f \frac{Y^n}{2} - f \frac{Y^P}{2}], 3 [4f \frac{Y^P}{2} - f \frac{Y^n}{2}] \right\} \tag{13}$$

The data show

$$f \frac{Y^P}{2} \geq f \frac{Y^n}{2} \text{ for all } x, \text{ so Eq. (13) can be simply written as}$$

$$0 \leq S(x) \leq 3 [4f \frac{Y^n}{2} - f \frac{Y^P}{2}] . \tag{14}$$

Inserting Eq. (12) into (10), we want to vary $S(x)$ subject to the inequality constraint (14). Introducing the inequality multiplier $\lambda(x)$, we consider the auxiliary functional

$$\mathcal{L} = F + \frac{2}{5} \int_{\tau}^1 \frac{dx}{x} \lambda(x) S(x) \left[3(4f \frac{Y^n}{2} - f \frac{Y^P}{2}) - S(x) \right] \tag{15}$$

where

$$F = \int_{\tau}^1 \frac{dx}{x} \left[\frac{4}{9} U(x) U(\tau/x) + \frac{1}{9} D(x) D(\tau/x) + \frac{1}{9} S(x) S(\tau/x) \right] \tag{16}$$

and where U and D are given by Eq. (12).

Then the variational derivative gives

$$\frac{\delta \mathcal{L}}{\delta S(x)} = \frac{2}{5x} \left\{ - f \frac{Y^P}{2} \left(\frac{\tau}{x} \right) + \frac{2}{3} S \left(\frac{\tau}{x} \right) + \lambda(x) \left[3(4f \frac{Y^n}{2} - f \frac{Y^P}{2}) - 2S(x) \right] \right\} = 0 \tag{17}$$

The rest of the analysis proceeds as in our first example in Sec. II.

The interior, when $0 < S(x) < 3(4f \frac{Y^n}{2} - f \frac{Y^p}{2})$, is even more easily disposed of than before, since in this case, $\lambda(x) = 0$ implies

$$S\left(\frac{\tau}{x}\right) = \frac{3}{2} f \frac{Y^p}{2}(\tau/x).$$

But, from (14) this implies

$$\frac{3}{2} f \frac{Y^p}{2} \leq 3(4f \frac{Y^n}{2} - f \frac{Y^p}{2}),$$

or simply

$$\frac{3}{8} \leq \frac{f \frac{Y^n}{2}}{f \frac{Y^p}{2}} \tag{18}$$

In fact, this last inequality does not seem to be satisfied anywhere by the data, so we may disregard this set. (We could also eliminate it by consideration of the second differential without reference to the data.)

We have then four remaining cases to examine

$$B_{00}: S(x) = S(\tau/x) = 0$$

$$B_{01}: S(x) = 0, \quad S\left(\frac{\tau}{x}\right) = 3 \left[4f \frac{Y^n}{2}(\tau/x) - f \frac{Y^p}{2}(\tau/x) \right]$$

$$B_{10}: S(x) = 3 \left[4f \frac{Y^n}{2}(x) - f \frac{Y^p}{2}(x) \right], \quad S(\tau/x) = 0$$

$$B_{11}: S(x) = 3 \left[4f \frac{Y^n}{2}(x) - f \frac{Y^p}{2}(x) \right], \quad S(\tau/x) = 3 \left[4f \frac{Y^n}{2}(\tau/x) - f \frac{Y^p}{2}(\tau/x) \right]$$

It is easy to check that B_{01} and B_{10} are incompatible with the requirements $\lambda(x) \geq 0$, but that B_{00} and B_{11} are acceptable. It turns out that both of

these sets, B_{00} and B_{11} , are local maxima and hence, both must be evaluated and the larger chosen to give the global maximum. Thus

$$Q^4 \frac{d\sigma}{dQ^2} \leq \frac{4}{9} \pi \alpha^2 \tau \int_{\tau}^1 \frac{dx}{x} M(x) \quad (19)$$

where

$$M(x) = \text{Max} \left\{ \begin{array}{l} \left\{ \begin{array}{l} \frac{4}{5} \left[f_2^{\text{yp}}(x) - f_2^{\text{yn}}(x) \right] \left[f_2^{\text{yp}}(\tau/x) - f_2^{\text{yn}}(\tau/x) \right] \\ + \frac{9}{5} f_2^{\text{yp}}(x) f_2^{\text{yp}}(\tau/x) \end{array} \right. \quad (B_{00}) \\ \left\{ \begin{array}{l} 4 \left[f_2^{\text{yp}}(x) - f_2^{\text{yn}}(x) \right] \left[f_2^{\text{yp}}(\tau/x) - f_2^{\text{yn}}(\tau/x) \right] \\ + \left[4 f_2^{\text{yn}}(x) - f_2^{\text{yp}}(x) \right] \left[4 f_2^{\text{yn}}(\tau/x) - f_2^{\text{yp}}(\tau/x) \right] \end{array} \right. \quad (B_{11}) \end{array} \right. \quad (20)$$

The first alternative (B_{00}) for the integrand corresponds to $S(x) = S(\tau/x) = 0$; the second (B_{11}), to $D(x) = D(\tau/x) = 0$. The upper bound so obtained has been evaluated from the SLAC data and is plotted in Fig. 1. (With uncolored quarks this upper bound would be a factor of 3 higher everywhere.) It is important to note that the doubly differential cross section,

$$\frac{d^2\sigma}{dQ^2 dq_L}$$

where q_L is the longitudinal momentum of the lepton pair is proportional to the integrand of the Drell-Yan formula.⁸ Hence, expression (20) when multiplied by the relevant kinematic factors provides an upper bound

on this cross section.

We would now like to compare our bound with the Brookhaven data. Since this experiment is done on a uranium target, we cannot directly compare our bound on $pp \rightarrow \mu^+ \mu^- X$ with it, since some of the time the incoming proton hits a neutron. Neglecting nuclear effects and treating the target as a mixture of non-interacting protons and neutrons, we can calculate an upper bound on $pn \rightarrow \mu^+ \mu^- X$, and take the weighted average of the two bounds as the bound on the Brookhaven process. Strictly speaking, this is not really the bound we want. Rather, we should bound the weighted average cross section on protons and neutrons, and not average the bounds on the proton and neutron cross sections. In some problems, these two quantities are identical, and in the problems considered here their difference is negligible. For this reason, and because the separate proton and neutron bounds will be useful in conjunction with experiments on other nuclear targets, we have chosen to proceed by averaging the bounds.

The derivation of the bound for $pn \rightarrow \mu^+ \mu^- X$ which is similar to the one discussed above is presented in Appendix B, and the result is plotted in Fig. 2. We then have for the upper bound of the per nucleon cross section on a nuclear target:

$$Q^4 \frac{d\sigma}{dQ^2} (pU \rightarrow \mu^+ \mu^- X) \leq \left(\frac{Z}{A}\right) Q^4 \frac{d\sigma}{dQ^2} (pp \rightarrow \mu^+ \mu^- X) + \left(\frac{N}{A}\right) Q^4 \frac{d\sigma}{dQ^2} (pn \rightarrow \mu^+ \mu^- X)$$

where, for Uranium, $Z = 92$, $N = 146$, and $A = 238$.

The Brookhaven data, as well as the upper bound is presented in Fig. 3. Curve A is the weighted average bound we have described. Curve B is the same bound, corrected for the detection efficiency of the Brookhaven experiment--that is, the fact the lepton pairs with a laboratory longitudinal momentum $< 12 \text{ GeV}/c$ are not detected. Curve C is the data. Notice that the upper bound falls substantially below the data over a rather wide range of τ . This means that the usual colored quark parton model cannot possibly explain this data. Furthermore, the bound derived using the uncolored quark parton model is only a factor of 3 larger and falls quite close to the data. Since the quark distributions which realize these bounds are rather unphysical (or at least unorthodox), the imposition of other constraints ought to lower the bounds even farther. Therefore, we proceed, in the next section, to investigate the bounds which result when we constrain the distributions (especially those of the antiquarks) by using neutrino data.

IV. THE INCLUSION OF NEUTRINO DATA

(A) Phenomonology

It is well known¹ that the quark model can be tested not only in electroproduction but also in the deep inelastic scattering of neutrinos and antineutrinos from protons and neutrons. Indeed, measurements of the latter weak processes will determine not only the validity of the model but also the actual values of each of the six quark distributions,

u, \bar{u} , d, \bar{d} , s and \bar{s} . Basic tests of the model can be made, in principle, from the fact that more than six experimentally measurable distributions are determined by the quark distributions. (For completeness, we have collected in Appendix C some kinematical relations for leptonproduction in the quark parton model.)

Unfortunately, the cross sections for these weak processes are so small that, even at NAL, it will be some time before such data are available. Just as at Gargamelle, the data will first be available on neutrino scattering from heavy nuclei. Eventually, $\nu p \rightarrow \mu^- X$ and $\nu p \rightarrow \mu^+ X$ will be measured in the 15' bubble chamber but, if neutral currents exist, then these cross sections will not be known until the detection efficiency for muons is significantly improved.¹² Consequently, it will be several years before the quark distributions are known and unique predictions can be made for $pp \rightarrow \mu^+ \mu^- X$.

Neutrino scattering from a nucleus of equal numbers of protons and neutrons allows one to determine (up to nuclear corrections) the sum $(\nu p \rightarrow \mu X) + (\nu n \rightarrow \mu X)$ and hence, $u + d$ and $(\bar{u} + \bar{d})$ may be approximately determined from the doubly differential cross section [see, e.g., Ref. (13)].

$$\frac{d\Sigma^{\nu d}}{dx dy} \equiv \frac{\pi}{G_{ME}^2} \left[\frac{d\sigma^{\nu p}}{dx dy} + \frac{d\sigma^{\nu n}}{dx dy} \right] = 2x \left[G_+^{\nu}(x)(1-y)^2 + G_-^{\nu}(x) \right] \quad (21)$$

$$G_+^{\nu} = \bar{u} + \bar{d} \quad , \quad G_-^{\nu} = (u+d)\cos^2 \theta_c + 2s \sin^2 \theta_c$$

$$x = \frac{-q^2}{2M\nu}, \quad y = \frac{\nu}{E}$$

where E = neutrino lab energy, $q^2 = (\nu - \mu)^2$ momentum transfer
and $\nu = E - \frac{E}{\mu}$ = lepton energy loss.

To the extent that we can neglect $S \sin^2 \theta_c$ antineutrinos provide a consistency check, since the quark and antiquark distributions are simply interchanged. Alternatively, given the data for the singly differential cross sections,

$$\frac{d\sigma^{\nu p}}{dx} + \frac{d\sigma^{\nu n}}{dx} \quad \text{and} \quad \frac{d\sigma^{\bar{\nu} p}}{dx} + \frac{d\sigma^{\bar{\nu} n}}{dx},$$

one can again determine $u + d$ and $\bar{u} + \bar{d}$. A first attempt to do this has been made at CERN using the Gargamelle heavy liquid bubble chamber. The values of $u + d$ and $\bar{u} + \bar{d}$ so obtained are reproduced in Fig. 4.¹³ These data, together with the SLAC electroproduction data, provide four constraints on the six quark distributions. So one can ask: What is the maximum rate allowed for $pp \rightarrow \mu^+ \mu^- X$ which is compatible with these four constraints plus positivity of the probability distributions? We shall solve this problem below, but the reader should remember that there are good reasons to doubt the validity of the distributions obtained from Gargamelle. Until better neutrino data are available, our discussion is primarily illustrative of how such a problem may be solved.

Before beginning the mathematical discussion, let us point out some objections to taking the distributions presented in Fig. 4 too seriously. In the first place, we are urged¹³ to consider the data as only preliminary, and there are clear indications that many of the events included in arriving at these distributions are not, in fact, in the scaling region. One certainly does not have scaling in x , and the curves are derived with the hope that the Bloom-Gilman variable x' allows one to smoothly extrapolate from the nonscaling region to the scaling limit. If, on the contrary, we accept the distributions given by Perkins as valid, we can combine them with the data from electroproduction¹⁰ to obtain the distributions $U = u + \bar{u}$, $D = d + \bar{d}$, and $S = s + \bar{s}$. (See Sec. B below for details.) The resulting probabilities times their momentum fraction x are presented in Fig. 5. One sees that, despite large errors, the strange quark distributions are systematically negative for $x \leq 0.35$ and for $x \geq 0.65$. This is another indication that we should not take the functions in Fig. 4 too literally. Furthermore, if one were to accept the suggestion of Figs. 4 and 5 that there are no \bar{u} or \bar{d} quarks for $x \geq 0.35$ and neither s nor \bar{s} for $x \geq 0.65$, then the predicted cross section for $pp \rightarrow \mu^+ \mu^- X$ would be zero for $\tau > (0.65)^2 = 0.42$.¹⁴ Consequently, the observation of any signal for $\tau \geq 0.4$ (as seen in Ref. 11) provides evidence that either the muon pairs have not scaled or the antiquark distributions suggested by Gargamelle data are simply too small.¹⁵

In the absence of reliable data, it may be useful to estimate how large the antiquarks must be by constructing a simple model. Suppose that, for $x \geq 0.5$, we can neglect strange quarks, and that the distributions for nonstrange quarks are given by $u(x) = C_u (1-x)^3$ and $d(x) = C_d (1-x)^3$, as expected from the Drell-Yan-West relation and the dipole falloff of the proton form factor. We suppose, also, that the antiquark distributions may be similarly parameterized: $\bar{u} = \bar{C}_u (1-x)^3$ and $\bar{d} = \bar{C}_d (1-x)^3$.¹⁶ (It seems likely that the ratios \bar{C}_u/C_u and \bar{C}_d/C_d would be small.¹⁷) For such a model, we find for $pp \rightarrow \mu^+ \mu^- X$ (with colored quarks)

$$Q^4 \frac{d\sigma}{dQ^2} = \frac{4\pi\alpha^2}{3} \left[\frac{1}{3} \left(\frac{4}{9} C_u \bar{C}_u + \frac{1}{9} C_d \bar{C}_d \right) \right] f(\tau), \quad (22)$$

where to a good approximation, the function $f(\tau)$ is given by the expression

$$f(\tau) = \frac{24}{105} \tau \frac{(1-\tau)^7}{(1+\tau)^4} \left[1 + \frac{10}{9} \left(\frac{1-\tau}{1+\tau} \right)^2 + \frac{35}{33} \left(\frac{1-\tau}{1+\tau} \right)^4 + \dots \right]. \quad (23)$$

Setting the bracket in Eq. (22) equal to one, we plot $\frac{4}{3} \pi \alpha^2 f(\tau)$ in Fig. 6.

One sees from the figure that, to account for the observed signal for $0.6 \leq \tau \leq 0.8$, it must be that the bracket in Eq. (22) is on the order of 0.1. To account for a quark distribution as indicated in Figs. 4 and 5, we would have to have $C_u + \bar{C}_u \approx 4$ and $C_d + \bar{C}_d \approx 1$. It then follows that we can neglect the down quarks and find a ratio $\bar{C}_u/C_u \approx 0.04$.

Hence, with only 4% antiquarks, the signal might be accounted for at large τ . At smaller τ , the model would require a ratio perhaps ten

times as large. This model illustrates what a sensitive measure of antiquarks lepton pair production is.

Before leaving this section, we reiterate that, for quite some time, the only neutrino data available will be in scattering from heavy nuclei, so that only the sums $u + d$ and $\bar{u} + \bar{d}$ will be known. The question we now turn to is the natural one: How do the additional constraints from such data restrict the upper bound for $pp \rightarrow \mu^+ \mu^- X$?

(B) Derivation of the Bound

In mathematical terms, our problem may be stated as follows: Given data on U , D , S , and $\bar{Q} \equiv \bar{u} + \bar{d}$, what is the maximum rate for $pp \rightarrow \mu^+ \mu^- X$, assuming this cross section is given by the Drell-Yan formula, Eq. (1)? The solution to this problem is logically straightforward but is not representable in an analytical, closed form for all functions U , D , S and \bar{Q} . Consequently, we will illustrate the technique with a specific, simplified representation of the data in mind, but the methods employed and problems encountered will be sufficiently general to enable one to solve the problem in any case. For our model, we choose the "data" given in Fig. 7. This "data" is chosen to essentially agree with the Gargamelle data for $x > 0.3$ but is modified for $x < 0.3$ to agree more closely with our theoretical prejudices.¹⁸ As remarked earlier, such a model for the data gives a cross section of zero for $\tau > 0.4$. For $\tau < 0.4$, the upper bound to which we shall be lead is plotted as curve A in Fig. 8. On the other hand, the bound is extremely

sensitive to the small magnitude of the antiquark distributions. If we relax the "data" somewhat and arbitrarily choose $S = \frac{1}{3}D$ and $\bar{Q} = \frac{1}{10}D$ for $x > 0.3$, then one obtains the bound labelled curve B in Fig. 8.

One of the complications of "data" such as that of Fig. 7 is that the four constraint equations are not all linearly independent for all x . The "data" of Fig. 7 naturally divides itself into three regions R_i defined as follows:¹⁹

$$R_1 = \{x \mid U, D, S, \bar{Q} \neq 0\}$$

$$R_2 = \{x \mid U, D, S \neq 0; \bar{Q} = 0\}$$

$$R_3 = \{x \mid U, D \neq 0; S = \bar{Q} = 0\}$$

In Region R_1 , we have 4 independent constraints on 6 unknown distributions. In region R_2 , we have $\bar{u} = \bar{d} = 0$ and 3 independent constraints on the remaining 4 unknowns $u, d, s,$ and \bar{s} . Indeed, we have simply $u = U, d = D$, so the only remaining ambiguity concerns the specification of the strange quark distributions. In region R_3 , we have $\bar{u} = \bar{d} = s = \bar{s} = 0$ and hence, $u = U$ and $d = D$. Thus there is no ambiguity at all. [The values of U and D here are precisely those given in Eq. (11).] In the region R_1 , there is the same ambiguity concerning strange quarks as in region R_2 and, in addition, a five-fold ambiguity among the nonstrange quarks. The logical alternatives are delineated in Table I, and, in the last column, we indicated which

alternatives are compatible with the data presented in Fig. 7. In the last case, V, no nonstrange distribution vanishes, and there remains an ambiguity in their values.

It is useful in the following to classify points in the interval $\tau \leq x \leq 1$ in pairs $(x, \tau/x)$. If $x \in R_i$ and $\tau/x \in R_j$, we will say that the pair $(x, \tau/x)$ is in the set $R_i \otimes R_j$. To avoid classifying each pair twice, we can without loss of generality, restrict x to the region $\sqrt{\tau} < x < 1$, so that $\tau < \frac{\tau}{x} < \sqrt{\tau}$. Then it is easy to classify pairs, depending on the value of τ and the various permissible ranges for x and τ/x . The classification so obtained is presented in Table II.

We will obtain the maximum by the method of Lagrange multipliers, but first it is convenient to abbreviate our notation. We abbreviate the first three constraints.

$$U = u + \bar{u}, \quad D = d + \bar{d} \quad S = s + \bar{s}$$

by

$$Q_i = q_i + \bar{q}_i \quad i = 1, 2, 3$$

and the fourth we choose to express as

$$\bar{Q} = \bar{u} + \bar{d}$$

Introducing Lagrange multipliers $\lambda_i, \bar{\lambda}$ (for the four equality constraints) and six inequality multipliers $\eta_i, \bar{\eta}_i \geq 0$ (for the positivity constraints $q_i, \bar{q}_i > 0$), we consider the auxiliary function

$$\mathcal{L} = F + \int \frac{dx}{x} \left\{ \sum_i e_i^2 \left[\lambda_i (Q_i - q_i - \bar{q}_i) + \eta_i q_i + \bar{\eta}_i \bar{q}_i \right] + \frac{\lambda}{9} (\bar{Q} - \bar{u} - \bar{d}) \right\} \quad (24)$$

having extracted the factor e_i^2/x from the definition of the multipliers

Here

$$F(\tau) = \sum_i \int_{\tau}^1 \frac{dx}{x} e_i^2 q_i(x) \bar{q}_i(\tau/x)$$

or

$$F(\tau) = \sum_i \int_{\sqrt{\tau}}^1 \frac{dx}{x} e_i^2 \left[q_i(x) \bar{q}_i(\tau/x) + q_i(\tau/x) \bar{q}_i(x) \right] \quad (25)$$

The latter form for F is more useful from the point of view of the classification of pairs $(x, \tau/x)$.²⁰

Then the variational equations become

$$\frac{\delta \mathcal{L}}{\delta q_i(x)} = \bar{q}_i(\tau/x) - \lambda_i(x) + \eta_i(x) = 0 \quad (26)$$

$$\frac{\delta \mathcal{L}}{\delta \bar{q}_i(x)} = q_i(\tau/x) - \lambda_i(x) - \frac{\bar{\lambda}_i(x)}{9e_i^2} + \bar{\eta}_i(x) = 0 \quad (27)$$

where we have introduced

$$\bar{\lambda}_i \equiv \begin{cases} \bar{\lambda} & i = u, d \\ 0 & i = s \end{cases} \quad (28)$$

In Appendix D, we discuss the second differential and tangent cone and will refer to it from time to time in order to identify certain critical points as saddle points rather than maxima.

The rest of the discussion concerning the values of the distributions is straightforward, but tedious. The reader uninterested in details can simply skip to Table III where the value of the integrand in each case is presented, and to the paragraph following Eq. (45) in the text.

Earlier, we indicated the possible values of the distribution functions for each of the three sets R_1 , R_2 , and R_3 . Given the distributions at x , we can use the variational equations, Eq. (26) and (27), to obtain necessary conditions on the distributions at the reciprocal point, τ/x . For example, $x \in R_2$ implies $u(x) = U(x)$, $d(x) = D(x)$ and, since u and d are non-zero, we must have $\eta_u(x) = \eta_d(x) = 0$, so that (from (26))

$$\bar{u}(\tau/x) = \lambda_U(x), \quad \bar{d}(\tau/x) = \lambda_D(x) \quad (29)$$

The case when $x \in R_1$ is more complicated, since we have the five possibilities indicated in Table I. (In this case, as in R_2 , the only constraint on the strange quarks is $s + \bar{s} = S$, so we postpone discussion of strange quarks until after discussing the non-strange distributions.)

We will restrict our discussion to the three cases allowed by Fig. 7 (I, III, and V) since the others will very likely be excluded by reliable data as well. In these three cases, we have $u \neq 0$, $d \neq 0$, and hence, $\eta_u = \eta_d = 0$. Consequently, we find, as in R_2 , that Eq. (29) holds. (Since $\bar{Q} = \bar{u} + \bar{d}$ at every point, only one of these two multipliers is independent.) For case I, we find that

$$\bar{\lambda}(x) = d(\tau/x) - \bar{d}(\tau/x)$$

$$\bar{\eta}_u(x) = \bar{u}(\tau/x) - u(\tau/x) + \frac{1}{4} [d(\tau/x) - \bar{d}(\tau/x)] \geq 0 \quad (30)$$

For Case III, we find

$$\frac{\bar{\lambda}(x)}{4} = u(\tau/x) - \bar{u}(\tau/x)$$

$$\bar{\eta}_d(x) = 4[u(\tau/x) - \bar{u}(\tau/x)] + \bar{d}(\tau/x) - d(\tau/x) \geq 0 \quad (31)$$

For case V, we find

$$\bar{\lambda}(x) = 4[u(\tau/x) - \bar{u}(\tau/x)] = d(\tau/x) - \bar{d}(\tau/x)$$

and

$$\begin{aligned} u &= \frac{1}{10} [6U + D - 2\bar{Q}] \geq 0 \\ \bar{u} &= \frac{1}{10} [4U - D + 2\bar{Q}] \geq 0 \\ d &= \frac{1}{10} [9D + 4U - 8\bar{Q}] \geq 0 \\ \bar{d} &= \frac{1}{10} [D - 4U + 8\bar{Q}] \geq 0 \end{aligned} \quad (32)$$

where the arguments of all the functions are evaluated at τ/x . Note how in each case, the hypothesis as to the values of the distributions at x has led to necessary inequalities involving the distributions at the reciprocal point, τ/x .

As remarked earlier, in sets other than R_3 , the strange quark distributions are ambiguous. We turn now to the resolution of this ambiguity. The only constraint is $s(x) + \bar{s}(x) = S(x)$. We must consider 3 cases:

Case A Suppose $\bar{s}(x) = 0, s(x) = S(x) > 0.$

Then $\eta_s(x) = 0 \Rightarrow \bar{s}(\tau/x) = x\lambda_s(x).$ Also,

$$x\bar{\eta}_s(x) = \bar{s}(\tau/x) - s(\tau/x) \geq 0. \quad (33)$$

Case B Suppose $s(x) = 0, \bar{s}(x) = S(x) > 0.$

Then $\bar{\eta}_s(x) = 0 \Rightarrow s(\tau/x) = x\lambda_s(x).$ Also

$$x\eta_s(x) = s(\tau/x) - \bar{s}(\tau/x) \geq 0. \quad (34)$$

Case C Suppose $s(x) \neq 0, \bar{s}(x) \neq 0.$

$$\eta_s(x) = \bar{\eta}_s(x) = 0 \rightarrow s(\tau/x) = \bar{s}(\tau/x) = x\lambda_s(x) = \frac{1}{2}S(\tau/x). \quad (35)$$

Let us now discuss the various sets $R_i \otimes R_j$; first, for strange quarks only. In sets $R_2 \otimes R_2, R_2 \otimes R_1,$ and $R_1 \otimes R_1,$ we must subdivide the possibilities for the strange quarks into sets denoted by the obvious notation, $A \otimes A, A \otimes B, A \otimes C,$ etc.

$A \otimes A$ is impossible, since $\tau/x \in A \Rightarrow x\bar{\eta}_s(x) = -S(\tau/x) \geq 0,$ which is not true. $A \otimes B$ is allowed, since $\tau/x \in B \Rightarrow x\bar{\eta}_s(x) = S(\tau/x) \geq 0.$

Similarly, one can show that $A \otimes C, B \otimes B, B \otimes C,$ are impossible but $B \otimes A,$ and $C \otimes C$ are allowed. However, as shown in Appendix D, $C \otimes C$ is only allowed by considerations of the first derivative, whereas the second differential can be positive, negative, or zero. Thus, $C \otimes C$ is a saddle point, not a maximum.

In summary, then, the only two possible maxima are $A \otimes B$ and $B \otimes A.$ It is unnecessary to distinguish these two possibilities, since in either case, the integrand takes the same value:

$$s(x) \bar{s}(\tau/x) + \bar{s}(x) s(\tau/x) = S(x) S(\tau/x).$$

Of course, in all cases other than these three, $R_2 \otimes R_2$, $R_2 \otimes R_1$, and $R_1 \otimes R_1$, the contribution from strange quarks to the maximum is zero.

Having resolved the ambiguity of the strange quarks, we turn to the somewhat more complicated question of the values of the nonstrange quark distributions. Clearly, for $R_3 \otimes R_3$ and $R_3 \otimes R_2$, the integrand is zero. For $R_3 \otimes R_1$, we will consider only the three cases I, III, and V, which are compatible with data like Fig. 7:

$$R_3 \otimes R_1 \text{ (I): } D(x) \geq 4U(x) \quad (36)$$

$$R_3 \otimes R_1 \text{ (III): } 4U(x) \geq D(x) \quad (37)$$

$$R_3 \otimes R_1 \text{ (V): } 4U(x) = D(x) \quad (38)$$

Clearly, there is no ambiguity remaining in the value of the integrand, since only the second case, $R_3 \otimes R_1$ (III), is compatible with Fig. 7.

The case $R_2 \otimes R_2$ is unique (for nonstrange quarks), so no further discussion is necessary. The case $R_2 \otimes R_1$ is more complicated; however, the constraints on the nonstrange quarks are precisely as in $R_3 \otimes R_1$. Finally, we come to the most complicated case, $R_1 \otimes R_1$, which subdivides into $R_1(J) \otimes R_1(K)$ ($J, K = I, III, \text{ or } V$).

$$R_1(I) \otimes R_1(I): \quad \bar{\eta}_u = -U + \frac{1}{4}D - \frac{1}{2}\bar{Q} \geq 0, \text{ at both } x \text{ and } \tau/x. \quad (39)$$

$$\begin{aligned}
 R_1(I) \otimes R_1(III): \quad \bar{\eta}_u(x) &= 2\bar{Q}(\tau/x) - U(\tau/x) + D(\tau/x) \geq 0 \\
 \bar{\eta}_u(\tau/x) &= 4U(x) = 2\bar{Q}(x) - D(x) \geq 0
 \end{aligned}
 \tag{40}$$

$$R_1(I) \otimes R_1(V): \quad 10\bar{u}(x) = 4U(x) - D(x) + 2\bar{Q}(x) = 0.
 \tag{41}$$

Of the three cases above, the first inequalities (39) are never satisfied in our model; the second inequalities (40) will be satisfied only for x sufficiently small. Given arbitrary functions, U , D , and \bar{Q} , the third case (41) will only be satisfied at isolated points and, hence, contribute to the maximum only on a set of measure zero. Similar remarks apply to $R_1(V) \otimes R_1(I)$. Mutatis mutandis, the case $R_1(III) \otimes R_1(I)$ will be applicable for τ/x sufficiently small. Unfortunately, the cases $R_1(I) \otimes R_1(III)$ and $R_1(III) \otimes R_1(I)$ are not mutually exclusive, i. e., it can be seen that, when

$$2\bar{Q} + \frac{1}{4}D \geq U \text{ at both } x \text{ and } \tau/x,
 \tag{42}$$

both sets of inequalities (40) are satisfied. We have no choice but to explicitly evaluate the integrand and choose the larger. We have

$$\sum_{i=u,d} e_i^2 [q_i(x)\bar{q}_i(\frac{\tau}{x}) + q_i(\frac{\tau}{x})\bar{q}_i(x)] \cdot \begin{cases} \frac{4}{9} U(x)\bar{Q}(\frac{\tau}{x}) + \frac{1}{9} \bar{Q}(x)D(\frac{\tau}{x}) \\ \text{in } R_1(I) \otimes R_1(III) \\ \frac{4}{9} \bar{Q}(x)U(\frac{\tau}{x}) + \frac{1}{9} D(x)\bar{Q}(\frac{\tau}{x}) \\ \text{in } R_1(III) \otimes R_1(I) \end{cases}
 \tag{43}$$

We next proceed to the case $R_1(\text{III}) \otimes R_1(\text{III})$: We find

$$\bar{\eta}_d = 4U - D - 8\bar{Q} > 0, \quad \text{at both } x \text{ and } \tau/x \quad (44)$$

[Note that this inequality is incompatible with (42).]

In $R_1(\text{III}) \otimes R_1(\text{V})$, we find

$$10\bar{d}(x) = D(x) - 4U(x) + 8\bar{Q}(x) = 0, \quad (45)$$

which will be satisfied, at most, at isolated points. Similar remarks apply to $R_1(\text{V}) \otimes R_1(\text{III})$.

The case $R_1(\text{V}) \otimes R_1(\text{V})$ would appear to be possible. However, it is a saddle point, (See Appendix B).

In summary, then, the only cases compatible with the "data" of Fig. 7 is $R_1(\text{I}) \otimes R_1(\text{III})$, $R_1(\text{III}) \otimes R_1(\text{I})$, and $R_1(\text{III}) \otimes R_1(\text{III})$. We present, in Table III, the value of the integrand in each case allowed by our model. The upper bound so computed is presented as curve A in Fig. 8. Note that it falls well below the data for almost all $x \geq 0$. Again we note that the integrand of our bound provides a bound on the doubly differential cross section.

Finally we would like to indicate how easily the preceding analysis may be applied to data which is somewhat different from that shown in Fig. 7. Consider, for example, data exactly like Fig. 7 for $x \leq 0.3$, but for $x \geq 0.3$, suppose $S = \frac{1}{3}D$ and $\bar{Q} = \frac{1}{10}D$. Choose U and D as

before. Thus, instead of being exactly zero, these distributions are quite small. Clearly, the pair $(x, \tau/x)$ is in $R_1 \otimes R_1$ for all points x . So the possible sets are those indicated in Table III for this class. For such data, the maximum is unambiguously given by $R_1(\text{III}) \otimes R_1(\text{III})$ for $x \geq 0.12$. The upper bound from such a model is also presented in Fig. 8 as the curve labelled B.

We should also remark that, for most input data, bounds such as the ones obtained above cannot be saturated by any distribution function; rather, the bound is the upper envelope produced by all possible distributions.

V. CONCLUSIONS

It seems clear from the preceding discussion that at least one of the following three statements must be correct.

1. The experimentally observed cross section per nucleon, N , is not the scaling limit for the process $pN \rightarrow \mu^+ \mu^- X$.
2. The Drell-Yan formula for $pp \rightarrow \mu^+ \mu^- X$ requires modification.
3. The colored quark-parton model is incorrect.

We discuss each possibility in turn:

(1) There are a number of effects which cause us to doubt that the data is the scaling limit of $pp \rightarrow \mu^+ \mu^- X$. First of all, the experiment was done on Uranium, and it is not at all clear how nuclear effects distort the cross section. For example, one ought to take into account absorption of the proton beam as it passes through the nucleus. It would

therefore be useful to do the experiment with several different nuclear targets in order to determine more precisely the significance of nuclear physics.²¹ Secondly, because the target is large, nearly all secondary mesons produced will interact, some of which will produce $\mu^+ \mu^-$ pairs. As x increases toward 1, the probability of finding an antiquark in a meson is, according to the common wisdom, much greater than in a proton; hence as τ increases, the contribution from processes such as $\pi p \rightarrow \mu^- \mu^+ X$ becomes relatively more important.²² Third, there is the possibility that scaling has not yet been reached for this process, and so similar experiments such as those planned and being carried out at NAL at other energies are very important. Finally, of course, it is possible that the $\mu^- \mu^+$ pair observed has nothing whatsoever to do with the process of heavy muon pair production. On this possibility, we have no comment.

(2) Consider now the possibility that the Drell-Yan formula is incorrect. This seems to us to likely, for strong interaction effects may very well modify the cross section.²³ Suppose, for a moment, that the only effect of strong interactions is to elastically scatter the partons forward. Then this would simply change the overall normalization of the Drell-Yan expression without altering its form.⁹ To the extent that the dominant contribution of strong interactions is diffraction scattering in a narrow forward cone, this would remain a good approximation. Thus, we might anticipate that the shape but not the magnitude of the

Drell-Yan formula is correct.²⁴ Unfortunately, it seems very unlikely that the shoulder seen in the data between $\tau = 0.1$ and $\tau = 0.3$ (see Fig. 3) could be accounted for in this way, as has been suggested.²⁵ We also want to remark that Feynman¹ takes a different point of view and argues that interactions among wees does not alter the probability of finding a hard parton, so the Drell-Yan formula is not modified by strong interactions.

(3) Third, we consider the possibility that the colored quark-parton model is incorrect. Certainly, an analysis of the type presented here should be performed for other constituent possibilities, such as the Han-Nambu model, or models with charmed particles. We suspect that the greater the mean-squared charge, the smaller the bound will be, so the situation will become even worse in most such models. There is also the possibility that the basic parton or free field approach to the light-cone simply is incorrect, at least for time-like photons. The data from SPEAR on $e^+e^- \rightarrow$ hadrons suggests that we should take this possibility seriously, but we prefer to wait until we have a better understanding of how scaling behavior should be approached.

In addition to the theoretical problems found generally in the parton model, it seems clear that the reliability of the Drell-Yan formula is an important area of theoretical investigation. Furthermore, it is clearly important to do lepton pair production experiments on a variety of targets over a wide kinematic range in order to get as good an under-

standing of this crucial process as possible. If we obtain more confidence in the theoretical underpinnings behind deep inelastic pair production, then we would suggest that a direct measurement of the doubly differential cross section for $pp \rightarrow \mu^- \mu^+ X$ may be much more sensitive to the antiquark distributions for large x than is a measurement of neutrino cross sections. In the muon pair production, the signal is directly proportional to the probability for finding antiquarks, whereas in the neutrino case, it must be obtained as the very small difference of neutrino and anti-neutrino cross sections.

In this paper we have tried to illustrate how a powerful technique can be used to obtain very general model independent bounds. Because of its intrinsic interest, we have considered heavy lepton pair production, but our approach clearly has a wide range of applications. For instance, a general study of bounds on neutrino cross sections imposed by the electroproduction data should be performed. In addition, these techniques can be applied to the exciting area of hadron production at large transverse momenta.

ACKNOWLEDGMENT

This work was completed while one of us (MBE) was a visitor at the California Institute of Technology. He would like to thank the members of the theoretical and phenomenology groups, in particular Prof. G. C. Fox for discussions and for their hospitality.

APPENDIX A

For a discussion of the tangent cone, we refer the reader to Ref. 7. Since our only constraints are $p(x) \geq 0$ and $p(x) \leq P(x)$, the tangent vectors $h(x)$ satisfy $h(x) = 0$ if $p(x) = 0$ or $p(x) = P(x)$

$h(x)$ arbitrary if $0 < p(x) < P(x)$

The only nonzero second differential is

$$\frac{\delta^2 \mathcal{L}}{\delta p(x) \delta p(y)} = -\frac{4}{x} \delta(y - \tau/x) \quad (\text{A1})$$

So

$$\mathcal{L}'' = -4 \int_{\tau}^1 \frac{dx}{x} h(x) h\left(\frac{\tau}{x}\right) \quad (\text{A2})$$

At a local maximum, $\mathcal{L}'' \leq 0$.

In the set I, for example, $h(x)$ and $h(\tau/x)$ are arbitrary so we can certainly choose them of opposite signs to give $\mathcal{L}'' > 0$. Hence, I cannot be a local maximum. ²⁶

APPENDIX B

For protons on neutrons, we must maximize

$$\begin{aligned}
F &= \int_{\tau}^1 \frac{dx}{x} \left\{ \frac{4}{9} \left[u(x) \bar{d}(\tau/x) + \bar{u}(x) d(\tau/x) \right] \right. \\
&+ \frac{4}{9} \left[d(x) \bar{u}(\tau/x) + \bar{d}(x) u(\tau/x) \right] + \frac{1}{9} \left[s(x) \bar{s}(\tau/x) + \bar{s}(x) s(\tau/x) \right] \left. \right\} \\
&= \int_{\tau}^1 \frac{dx}{x} \left[\frac{5}{9} \left[u(x) \bar{d}(\tau/x) + \bar{u}(x) d(\tau/x) \right] + \frac{2}{9} s(x) \bar{s}(\tau/x) \right] \\
&= \int_{\sqrt{\tau}}^1 \left\{ \frac{dx}{x} \left[\frac{5}{9} \left(u(x) \bar{d}(\tau/x) + \bar{d}(x) u(\tau/x) + \bar{u}(x) d(\tau/x) + d(\tau/x) \bar{u}(\tau/x) \right) \right] \right. \\
&\quad \left. + \frac{2}{9} \left(s(x) \bar{s}(\tau/x) + s(\tau/x) \bar{s}(x) \right) \right\} \quad (B1)
\end{aligned}$$

subject to the three constraints $u + \bar{u} = U$, $d + \bar{d} = D$, $s + \bar{s} = S$ plus six positivity constraints.

The strange quark problem is precisely as before, but the non-strange quarks differ. Neglecting strange quarks for the moment, consider

$$\mathcal{L} = F + \frac{5}{9} \int \frac{dx}{x} \lambda_U(x) (U - u - \bar{u}) + \lambda_D (D - d - \bar{d}) + \eta_u u + \bar{\eta}_u \bar{u} + \eta_d d + \bar{\eta}_d \bar{d} \quad (B2)$$

we have

$$\frac{\delta \mathcal{L}}{\delta u(x)} = \frac{5}{9x} \left[\bar{d}(\tau/x) + \lambda_U(x) + \eta_u(x) \right] = 0$$

$$\begin{aligned}\frac{\delta \mathcal{L}}{\delta d(x)} &= \frac{5}{9x} \left[\bar{u}(\tau/x) + \lambda_D(x) + \eta_d(x) \right] = 0 \\ \frac{\delta \mathcal{L}}{\delta \bar{u}(x)} &= \frac{5}{9x} \left[d(\tau/x) + \lambda_U(x) + \bar{\eta}_u(x) \right] = 0 \quad (\text{B3}) \\ \frac{\delta \mathcal{L}}{\delta \bar{d}(x)} &= \frac{5}{9x} \left[u(\tau/x) + \lambda_D(x) + \bar{\eta}_d(x) \right] = 0\end{aligned}$$

As before, the interior can be ruled out. If $u(x) \neq 0$, $\bar{u}(x) \neq 0$, then $\eta_u(x) = \bar{\eta}_u(x) = 0 \Rightarrow d(\tau/x) = \bar{d}(\tau/x) = \frac{1}{2}D(\tau/x) \Rightarrow \eta_d(\tau/x) = \bar{\eta}_d(\tau/x) = 0 \Rightarrow u(x) = \bar{u}(x) = \frac{1}{2}U(x)$. Thus, if u and \bar{u} are in the interior at x , then d and \bar{d} are in the interior at τ/x . Consideration of the second differential on the tangent cone shows that this case is a saddle point.

Next, consider boundary cases:

$$\begin{aligned}\bar{u} = 0, u = U &\Rightarrow \bar{\eta}_u(x) = \bar{d}(\tau/x) - d(\tau/x) \geq 0 \\ u = 0, \bar{u} = \bar{U} &\Rightarrow \eta_u(x) = d(\tau/x) - \bar{d}(\tau/x) \geq 0 \\ \bar{d} = 0, d = D &\Rightarrow \bar{\eta}_d(x) = \bar{u}(\tau/x) - u(\tau/x) \geq 0 \\ d = 0, \bar{d} = \bar{D} &\Rightarrow \eta_d(x) = u(\tau/x) - \bar{u}(\tau/x) \geq 0\end{aligned} \quad (\text{B4})$$

Consideration of these inequalities leads to the conclusion that only four sets are allowed for the pair $(x, \tau/x)$

1. $\bar{u} = \bar{d} = 0$ at x , $u = d = 0$ at τ/x
2. $u = d = 0$ at x , $\bar{u} = \bar{d} = 0$ at τ/x
3. $\bar{u} = d = 0$ at x , $u = \bar{d} = 0$ at τ/x

$$4. \quad u = \bar{d} = 0 \text{ at } x, \quad \bar{u} = d = 0 \text{ at } \tau/x$$

For all four of these cases, the value of the integrand is the same:

Restoring strange quarks, we find the value of the maximum is

$$F = \int_{\sqrt{\tau}}^1 \frac{dx}{x} \left\{ \frac{5}{9} \left[U(x) D(\tau/x) + D(x) U(\tau/x) \right] + \frac{2}{9} S(x) S(\tau/x) \right\} \quad (B5)$$

If $S(x) = 0$ for all x , U and D are given by Eq. (11). We evaluate this case and plot it in Fig. 2 as the dashed line. Next, we want to maximize Eq. (B5) with respect to S , where U and D are given in terms of S by Eq. (12). This analysis proceeds essentially as in Eqs. (15) through (19). We find that, provided $f_2^n/f_2^p > 11/35$, only B_{00} and B_{11} are allowed, so that the maximum is given by

$$F = \int_{\tau}^1 \frac{dx}{x} M_n(x), \text{ where} \quad (B6)$$

$$M_n(x) = \text{Max} \begin{cases} \frac{1}{10} \left[4f_2^{yn}(x) - f_2^{yp}(x) \right] \left[4f_2^{yn}(\tau/x) - f_2^{yp}(\tau/x) \right] \\ + \left[f_2^{yn}(x) - f_2^{yp}(x) \right] \left[4f_2^{yp}(\tau/x) - f_2^{yn}(\tau/x) \right] \quad (B_{00}) \\ \left[4f_2^{yn}(x) - f_2^{yp}(x) \right] \left[4f_2^{yn}(\tau/x) - f_2^{yp}(\tau/x) \right] \quad (B_{11}) \end{cases}$$

We evaluate this and plot it as the solid line in Fig. 2. We see that the proton-neutron bound falls well below the proton-proton bound.

If we can neglect effects due to binding of nucleons, then a nucleus

of Z protons and N neutrons ($N + Z = A$) will have an average cross section per nucleon equal to

$$\left(\frac{Z}{A}\right) (\text{pp} \rightarrow \mu^+ \mu^- X) + \left(\frac{N}{A}\right) (\text{pn} \rightarrow \mu^+ \mu^- X) \quad (\text{B7})$$

For the Uranium target used in the Brookhaven experiment,¹¹ we have $Z = 92$, $N = 146$, $A = 238$ so there is a considerable neutron excess. The upper bound on the average cross section per nucleon can be computed from Eq. (B7) and from the curves B in Figs. (1) and (2). This bound is plotted in Fig. (3) against the Brookhaven data.

APPENDIX C

We summarize below formulas for neutrino interactions in the quark model. With spin $\frac{1}{2}$ quarks only, $\nu N \rightarrow \mu^- X$ and $\bar{\nu} N \rightarrow \mu^+ X$ have scaling forms:

$$\frac{d\sigma}{dx dy} = \frac{G^2 ME}{\pi} 2x [G_+(x)(1-y)^2 + G_-(x)]$$

Proton

$$G_+^{\nu p} = \bar{u}$$

$$G_+^{\bar{\nu} p} = u$$

$$G_-^{\nu p} = d \cos^2 \theta_c + s \sin^2 \theta_c$$

$$G_-^{\bar{\nu} p} = \bar{d} \cos^2 \theta_c + \bar{s} \sin^2 \theta_c$$

Neutron

$$G_+^{\nu n} = \bar{d}$$

$$G_+^{\bar{\nu} n} = d$$

$$G_-^{\nu n} = u \cos^2 \theta_c + s \sin^2 \theta_c$$

$$G_-^{\bar{\nu} n} = \bar{u} \cos^2 \theta_c + \bar{s} \sin^2 \theta_c$$

Sum of proton plus neutron: $G_i^j \equiv G_i^{jp} + G_i^{jn}$, $i = +, -; j = \nu, \bar{\nu}$

$$G_+^{\nu} = \bar{u} + \bar{d}$$

$$G_+^{\bar{\nu}} = u + d$$

$$G_-^{\nu} = (u+d) \cos^2 \theta_c + 2s \sin^2 \theta_c$$

$$G_-^{\bar{\nu}} = (\bar{u} + \bar{d}) \cos^2 \theta_c + 2\bar{s} \sin^2 \theta_c$$

Sum of neutrino plus antineutrino: $G_i = G_i^{\nu} + G_i^{\bar{\nu}}$, $i = +, -$

$$G_+ = U + D$$

$$G_- = (U+D) \cos^2 \theta_c + 2S \sin^2 \theta_c$$

Electroproduction Scaling Functions:

$$\frac{\nu W_2^{\gamma p}}{x} = f \frac{\gamma p}{2} = \frac{4}{9}U + \frac{1}{9}D + \frac{1}{9}S \quad \frac{\nu W_2^{\gamma n}}{x} = f \frac{\gamma n}{2} = \frac{4}{9}D + \frac{1}{9}U + \frac{1}{9}S$$

$$\text{sum of proton plus neutron: } f \frac{\gamma}{2} \equiv f \frac{\gamma p}{2} + f \frac{\gamma n}{2} = \frac{5}{9}(U+D) + \frac{2}{9}S$$

Inverting:

$$U + D = G_+ \quad S = \frac{9}{2}f \frac{\gamma}{2} - \frac{5}{2}G_+$$

$$U = \frac{1}{2}G_+ + \frac{3}{2}(f \frac{\gamma p}{2} - f \frac{\gamma n}{2})$$

$$D = \frac{1}{2}G_+ - \frac{3}{2}(f \frac{\gamma p}{2} - f \frac{\gamma n}{2})$$

Constraints:

$$G_+ - G_- = (6G_+ - 9f \frac{\gamma}{2}) \sin^2 \theta_c$$

$$G_-^{\nu p} - G_-^{\nu n} = (G_+^{\bar{\nu} n} - G_+^{\bar{\nu} p}) \cos^2 \theta_c$$

$$G_-^{\bar{\nu} p} - G_-^{\nu n} = (G_+^{\nu n} - G_+^{\nu p}) \cos^2 \theta_c$$

Singly Differential Cross Section:

$$\frac{d\sigma^{jk}}{dx} = \frac{G_{ME}^2}{\pi} \frac{8x}{3} G^{jk}$$

where

$$G^{jk} = \frac{1}{4}G_+^{jk} + \frac{3}{4}G_-^{jk} \quad j = \nu, \bar{\nu}; \quad k = p, n$$

$$\text{Sum of proton plus neutron: } G^j = G^{jp} + G^{jn} \quad j = \nu, \bar{\nu}$$

Knowledge of $f \frac{\gamma}{2}$ and $G^{\nu} + G^{\bar{\nu}}$ determines $U + D$ and S :

$$U + D = \left(1 - \frac{9}{2} \sin^2 \theta_c\right)^{-1} \left[G^\nu + G^{\bar{\nu}} - \frac{27}{4} \sin^2 \theta_c f \frac{Y}{2}\right]$$

$$S = \left(1 - \frac{9}{2} \sin^2 \theta_c\right)^{-1} \left[\frac{9}{2} \left(1 - \frac{3}{4} \sin^2 \theta_c\right) f \frac{Y}{2} - \frac{5}{2} (G^\nu + G^{\bar{\nu}})\right]$$

Note also

$$u + d = \left(\frac{4}{9 \cos^2 \theta_c - 1}\right) \left[3 G^\nu \cos^2 \theta_c - G^{\bar{\nu}} + \frac{3}{2} (\bar{s} - 3 \cos^2 \theta_c s) \sin^2 \theta_c\right]$$

$$\bar{u} + \bar{d} = \left(\frac{4}{9 \cos^2 \theta_c - 1}\right) \left[3 G^{\bar{\nu}} \cos^2 \theta_c - G^\nu + \frac{3}{2} (s - 3 \cos^2 \theta_c \bar{s}) \sin^2 \theta_c\right]$$

In limit $\theta_c = 0$,

$$u + d = \frac{1}{2} \left[3G^\nu - G^{\bar{\nu}}\right]$$

$$\bar{u} + \bar{d} = \frac{1}{2} \left[3G^{\bar{\nu}} - G^\nu\right]$$

$$U + D = G^\nu + G^{\bar{\nu}}$$

APPENDIX D

The only non-zero second derivative is

$$\frac{\delta^2 \mathcal{L}}{\delta q_i(x) \delta \bar{q}_i(y)} = \frac{e_i^2}{x} \delta(y - \frac{\tau}{x}) \quad (D1)$$

The tangent cone is determined from the constraint equations.

Corresponding to the six distributions $u, \bar{u}, d, \bar{d}, s, \bar{s}$, we identify components of a tangent vector $h = (h_u, \bar{h}_u, h_d, \bar{h}_d, h_s, \bar{h}_s)$. The four equality constraints lead to the four conditions.

$$\begin{aligned} h_i(x) + \bar{h}_i(x) &= 0 \quad i = u, d, s \\ \bar{h}_u(x) + \bar{h}_d(x) &= 0. \end{aligned} \quad (D2)$$

Hence the tangent cone is, at most, two dimensional.

The second differential is

$$\begin{aligned} \mathcal{L}'' &= \sum_{i,j} \int_{\tau}^1 h_i(x) \frac{\delta^2 \mathcal{L}}{\delta q_i(x) \delta \bar{q}_j(y)} h_j(y) dx dy = \\ &= \sum_i e_i^2 \int_{\tau}^1 \frac{dx}{x} h_i(x) \bar{h}_i(\tau/x) \end{aligned} \quad (D3)$$

If we choose $h_d(x), h_s(x)$ as independent components and eliminate the other four components in their favor, we find

$$\mathcal{L}'' = -\frac{1}{9} \int_{\tau}^1 \frac{dx}{x} \left[5h_d(x)h_d\left(\frac{\tau}{x}\right) + h_s(x)h_s\left(\frac{\tau}{x}\right) \right] \quad (D4)$$

Whenever one of the inequality constraints, $q_i(x) \geq 0$, $\bar{q}_i(x) \geq 0$, becomes an equality, then there is an additional constraint on the tangent cone. Specifically, whenever $q_i(x) = 0$, we must have $h_i(x) = 0$.

In the text, we remark that, for strange quarks, the case $C \otimes C$ is a saddle point. To see this is easy, for, since neither s nor \bar{s} vanishes at x or τ/x , we can choose the independent component h_s arbitrarily at both x and τ/x . Consequently, we may choose all other components of the tangent vector to be zero and choose $h_s(x)$, $h_s(\tau/x)$ to give $\mathcal{L}'' = - \int \frac{dx}{x} h_s(x) h_s(\tau/x) > 0$.²⁶ Hence $C \otimes C$ cannot be a local maximum.

The case $R_1(V) \otimes R_1(V)$ has $u, \bar{u}, d, \bar{d} \neq 0$ at both x and τ/x . Hence, one can choose non-zero independent components $h_d(x)$, $\bar{h}_d(\tau/x)$, such that $\mathcal{L}'' > 0$, so this case is also not a maximum.

TABLE I

Alternatives for Region R_1

Case	u	\bar{u}	d	\bar{d}	Consistent with Model
I	U	0	$D - \bar{Q}$	\bar{Q}	Yes
II	0	U	$D + U - \bar{Q}$	$\bar{Q} - U$	No ($\bar{d} < 0$)
III	$U - \bar{Q}$	\bar{Q}	D	0	Yes
IV	$U + D - \bar{Q}$	$\bar{Q} - D$	0	D	No ($u < 0$)
V	$\neq 0$	$\neq 0$	$\neq 0$	$\neq 0$	Sometimes

In all cases, we have $s + \bar{s} = S$.

TABLE II

Range of τ		Subdivision				Class	
$a < \tau < b$		$x_1 < x < x_2$		$\tau/x_2 < \tau/x < \tau/x_1$			
a	b	x_1	x_2	τ/x_2	τ/x_1		
1.	0.6	1	τ	1	τ	$R_3 \boxtimes R_3$	
2.	0.36	0.6	$\tau/0.6$	1	τ	0.6	$R_3 \boxtimes R_2$
			$\sqrt{\tau}$	0.6	$\tau/0.6$	$\sqrt{\tau}$	$R_2 \boxtimes R_2$
3.	0.3	0.36	0.6	1	τ	$\tau/0.6$	$R_3 \boxtimes R_2$
			$\sqrt{\tau}$	0.6	$\tau/0.6$	$\sqrt{\tau}$	$R_2 \boxtimes R_2$
4.	0.18	0.3	$\tau/0.3$	1	τ	0.3	$R_3 \boxtimes R_1$
			0.6	$\tau/0.3$	0.3	$\tau/0.6$	$R_3 \boxtimes R_2$
			$\sqrt{\tau}$	0.6	$\tau/0.6$	$\sqrt{\tau}$	$R_2 \boxtimes R_2$
5.	0.09	0.18	0.6	1	τ	$\tau/0.6$	$R_3 \boxtimes R_1$
			$\tau/0.3$	0.6	$\tau/0.6$	0.3	$R_2 \boxtimes R_1$
			$\sqrt{\tau}$	$\tau/0.3$	0.3	$\sqrt{\tau}$	$R_2 \boxtimes R_2$
6.	0	0.09	0.6	1	τ	$\tau/0.6$	$R_3 \boxtimes R_1$
			0.3	0.6	$\tau/0.6$	$\tau/0.3$	$R_2 \boxtimes R_1$
			$\sqrt{\tau}$	0.3	$\tau/0.3$	$\sqrt{\tau}$	$R_1 \boxtimes R_1$

TABLE III

Value of Integrand in Permissible Cases

(We suppose $\sqrt{\tau} \leq x \leq 1$ in the following.)

<u>Case</u>	<u>Value of Integrand</u>
$R_3 \otimes R_3$	0
$R_3 \otimes R_2$	0
$R_2 \otimes R_2$	$\frac{1}{9} S(x) S(\tau/x)$
$R_2 \otimes R_1$	$\frac{4}{9} U(x) \bar{Q}(\tau/x) + \frac{1}{9} S(x) S(\tau/x)$
$R_3 \otimes R_1$	$\frac{4}{9} U(x) \bar{Q}(\tau/x)$
$R_1 \otimes R_1$	MAX+ S(x)S(τ/x)

The value of the maximum MAX is determined as follows:

(1) If $U \geq 2\bar{Q} + \frac{1}{4} D$ at x and τ/x , then we choose case $R_1(III) \otimes R_1(III)$

where

$$MAX = \frac{4}{9} \left[U(x) - \bar{Q}(x) \right] \bar{Q}(\tau/x) + \frac{4}{9} \bar{Q}(x) \left[U(\tau/x) - \bar{Q}(\tau/x) \right]$$

(2) If $U \leq 2\bar{Q} + \frac{1}{4} D$ at x } , then choose $R_1(III) \otimes R_1(I)$ where
 $U \geq 2\bar{Q} + \frac{1}{9} D$ at τ/x }

$$MAX = \frac{1}{9} D(x) \bar{Q}(\tau/x) + \frac{4}{9} \bar{Q}(x) U(\tau/x)$$

(3) If $U > 2\bar{Q} + \frac{1}{4} D$ at x } , then choose $R_1(I) \otimes R_1(III)$ where
 $U < 2\bar{Q} + \frac{1}{4} D$ at τ/x }

$$MAX = \frac{1}{9} \bar{Q}(x) D(\tau/x) + \frac{4}{9} U(x) \bar{Q}(\tau/x)$$

TABLE III (Contd.)

If $U \leq 2\bar{Q} + \frac{1}{4}D$ at both x and τ/x , choose the larger of the two values of MAX given in (2) and (3) above.

REFERENCES AND FOOTNOTES

- ¹R. P. Feynman, Photon-Hadron Interactions, 1972; W. A. Benjamin, Inc., Reading Mass.
- ²Some reviews are P. V. Landshoff and J. C. Polkinghorne, *Physics Reports* 5C, No. 1 (October 1972); R. Savit, in *AIP-Conference Proceedings* No. 14 (1973) ed. H. H. Bingham, et al., p. 639, and SLAC-Pub-1324; S. J. Brodsky in *AIP Conference Proceedings* No. 15, ed. C. Quigg (1973), p. 275.
- ³Even the relaxation of this assumption is occasionally entertained. See M. Chanowitz and S. D. Drell, *Phys. Rev. Letters* 30, 807 (1973).
- ⁴In addition to Ref. 1, see O. Nachtmann, *Phys. Rev.* D5, 686 (1972). *Phys. Rev.* D7, 3340 (1973), and *Nucl. Phys.* B38, 397 (1973).
- ⁵See the remarks on page 152 on Ref. 1.
- ⁶Recent examples of such constructions may be found in R. McElhaney and S. F. Tuan, "Some Aspects of the Quark Parton Model." V. Barger, "Two-Component Dual Parton-Regge Model of Deep Inelastic Electron and Neutrino Structure Functions," U. of Wisconsin Preprint, G. R. Farrar, CalTech Preprint CALT-68-422. H. Paar and M. Paschos, NAL preprint NAL-Pub-74/29-THY.
- ⁷M. B. Einhorn and R. Blankenbecler, *Ann. Phys.* 67, 480 (1971).
- ⁸S. D. Drell and T. M. Yan, *Phys. Rev. Letters* 25, 316 (1970), *Ann Phys.* 66, 478 (1971).

- ⁹Landshoff and Polkinghorne (Ref. 2) indicate a specific correction but have no way to calculate its effects.
- ¹⁰A. Bodek, Ph.D. Thesis, MIT, LNS Report No. COO-3069-116 (1972); E. M. Riordan, Ph.D. Thesis, MIT, LNS Report No. COO-3069-176 (1973).
- ¹¹J. H. Christenson, et al., Phys. Rev. D8, 2016 (1973).
- ¹²Even then, as discussed below, it will require extremely precise experiments to determine the strange quark distributions, s and \bar{s} , and, in any case, it will be difficult to determine the small anti-quark distributions \bar{u} and \bar{d} expected for large values of x .
- ¹³D. H. Perkins, Experimental Aspects of Neutrino Interactions, Oxford University Preprint, Ref. 67-73. We emphasize that the "data" is presented for illustration only and is not to be taken too seriously, inasmuch as further systematic corrections remain to be made. In solving the problem, it is useful to have specific data in mind.
- ¹⁴This comes about as follows: Obviously, there can be no contribution from nonstrange quarks for $\tau \geq 0.35$. Since either x or τ/x is greater than $\sqrt{\tau}$, there can be no contribution from strange quarks for $\sqrt{\tau} \geq 0.65$.
- ¹⁵The fact that the antiquarks necessary to explain the data would be relatively larger than expected was already suggested by the electroproduction bound.

¹⁶Other authors⁶ generally neglect antiquarks altogether or assume that the ratio of antiquarks to quarks vanishes rapidly as $x \rightarrow 1$. However, it has recently been suggested¹⁷ that the behavior of antiquarks is essentially the same as quarks.

¹⁷M. B. Einhorn and G. C. Fox, in preparation. The physical reason for this is simply that there is a virtual pion cloud around a proton. Assuming (a) that pions have a distribution of antiquarks vanishing like $(1-x)$ and (b) the probability of finding a pion in a proton for x near 1 is proportional to the single-particle inclusive distribution for pions $(1-x)^{1-2\alpha_\Delta(0)}$ (up to logarithms), the result follows from $\alpha_\Delta \approx 0$.

¹⁸Some of these prejudices include (approximate) SU_3 symmetry at $x = 0$ and positivity for all probability distributions.

¹⁹One could, in principle, avoid such a partition by giving S and \bar{Q} arbitrarily small but finite values in the regions where they vanish.

²⁰According to Eq. (1), the relation between this F and the cross section is simply $Q^4 \frac{d\sigma}{dQ^2} = \frac{4}{9} \pi \alpha^2 \int_0^1 F(\tau) d\tau$ for colored quarks and three times the right hand side for uncolored quarks.

²¹One of us (MBE) thanks Prof. M. Bander for emphasizing this point to him.

- ²²Using the inclusive data for $pN \rightarrow \pi X$ and the model of Farrar (Ref. 6) for the antiquark distribution in the pion, one can estimate this effect. It seems to be well below the observed signal strength for the range of τ covered in the Brookhaven experiment. (G.R. Farrar and G.C. Fox, unpublished.)
- ²³One might choose to believe only those predictions of the parton model which are derivable from the approach of operator commutators on the light cone. It seems that omission of strong interaction effects would lead to light-cone dominance for this process.
- ²⁴From usual considerations of the parton model, such final state (Pomeron) interactions seem to be required. The reason is that the Pomeron is just a representation for interactions among the wees, and without such interactions there is no way to smooth out the rapidity plateau produced by the remaining pieces of the incident hadrons. This point will be discussed further elsewhere.
- ²⁵R. W. Fidler, Physics Letters 46B, 455 (1973).
- ²⁶Strictly speaking, it is necessary that the interior I be of positive measure in order to give $\mathcal{L}'' > 0$. However, if I has zero measure, it will not contribute to the bound and so is of no consequence.

FIGURE CAPTIONS

- Fig. 1 Upper bound for $pp \rightarrow \mu^+ \mu^- X$ assuming a knowledge of νW_2 for protons and neutrons (solid line). The dashed line is the bound with the additional constraint that $s(x) = \bar{s}(x) = 0$.
- Fig. 2 Same as Fig. 1, for the process $pn \rightarrow \mu^+ \mu^- X$.
- Fig. 3 (A) Upper bound for process $pU \rightarrow \mu^+ \mu^- X$ calculated as a weighted average as described in the text.
(B) Same bound corrected to include detection efficiency at BNL.
(C) 28 GeV/c data from Brookhaven (Ref. 11).
- Fig. 4 Momentum fraction carried by quarks ($u + d$) and antiquarks ($\bar{u} + \bar{d}$). (Taken from Fig. 4.23 of Ref. 13.)
- Fig. 5 Momentum fraction carried by each species of quark x_U , x_D , and x_S . (Deduced from Fig. 4 and data from Ref. 10.)
- Fig. 6 The simple model of Eq. (22) and (23) (dashed line) for the behavior of the muon pair cross

section for large τ compared with the
Brookhaven data.

Fig. 7 Distributions for U, D, S and \bar{Q} motivated by
the Gargamelle data.

Fig. 8 Upper bound (A) obtained from electroproduction
data plus Fig. 7. Upper bound (B) obtained
by relaxing conditions on antiquarks. (See text
for discussion.)

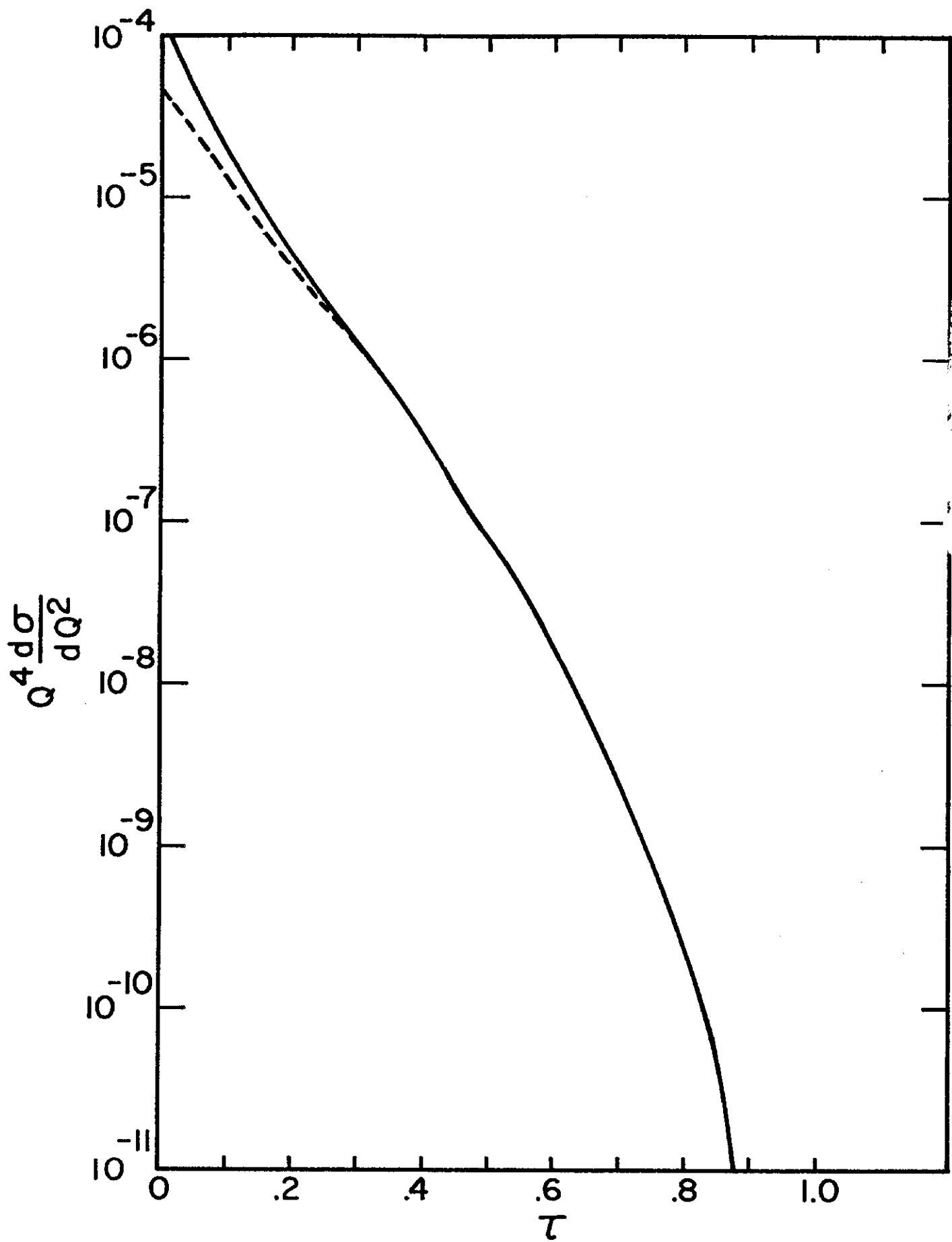


Figure 1

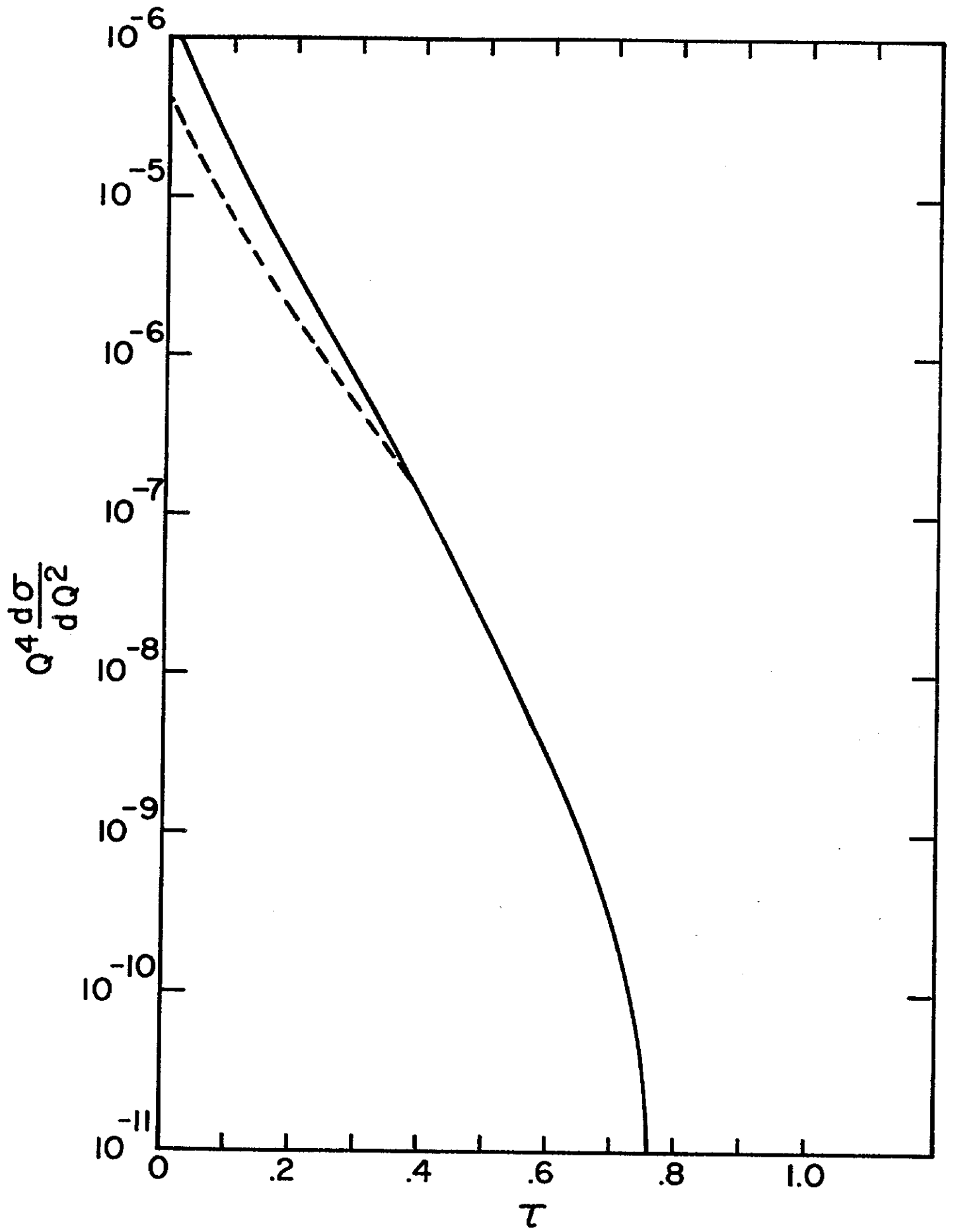


Figure 2

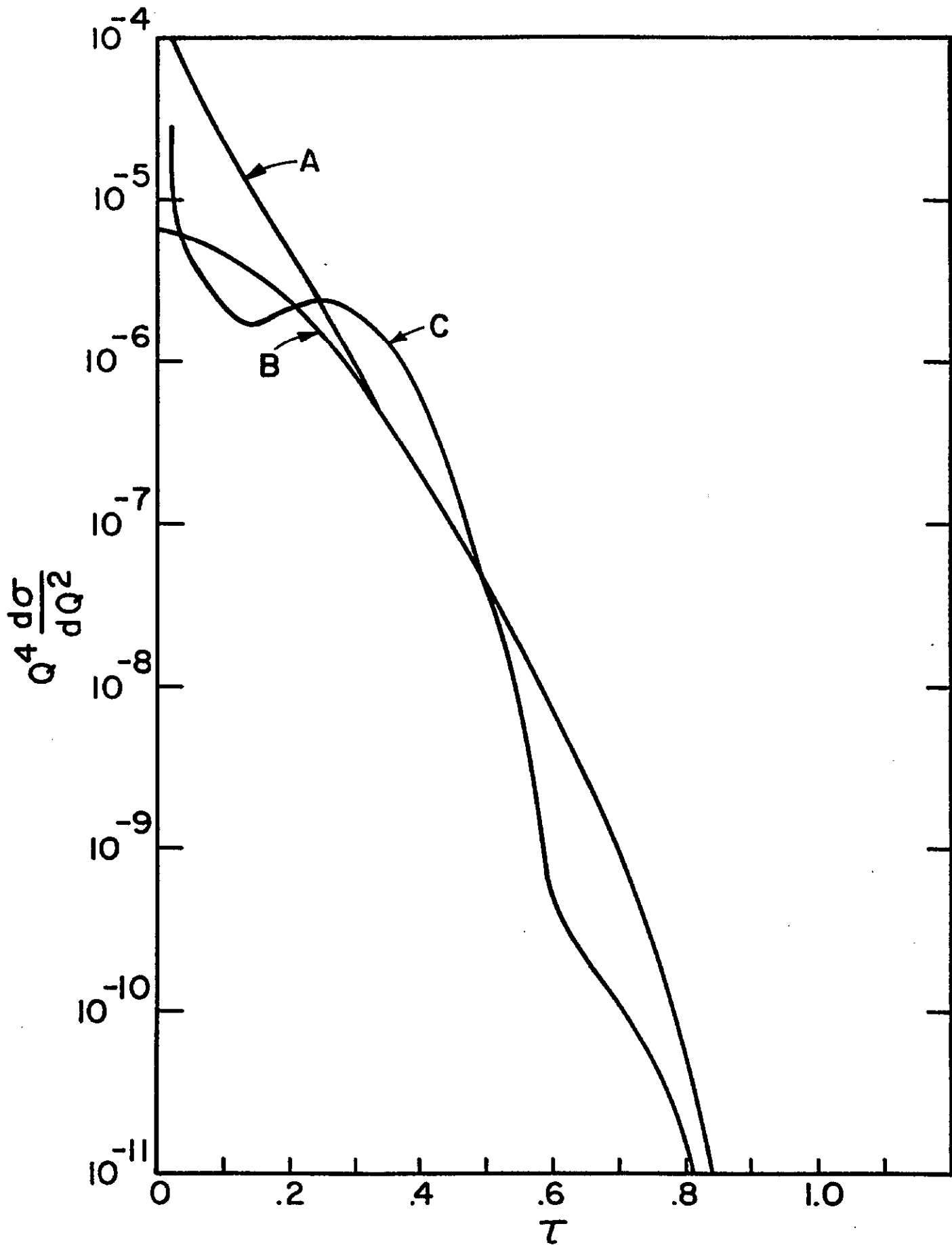


Figure 3

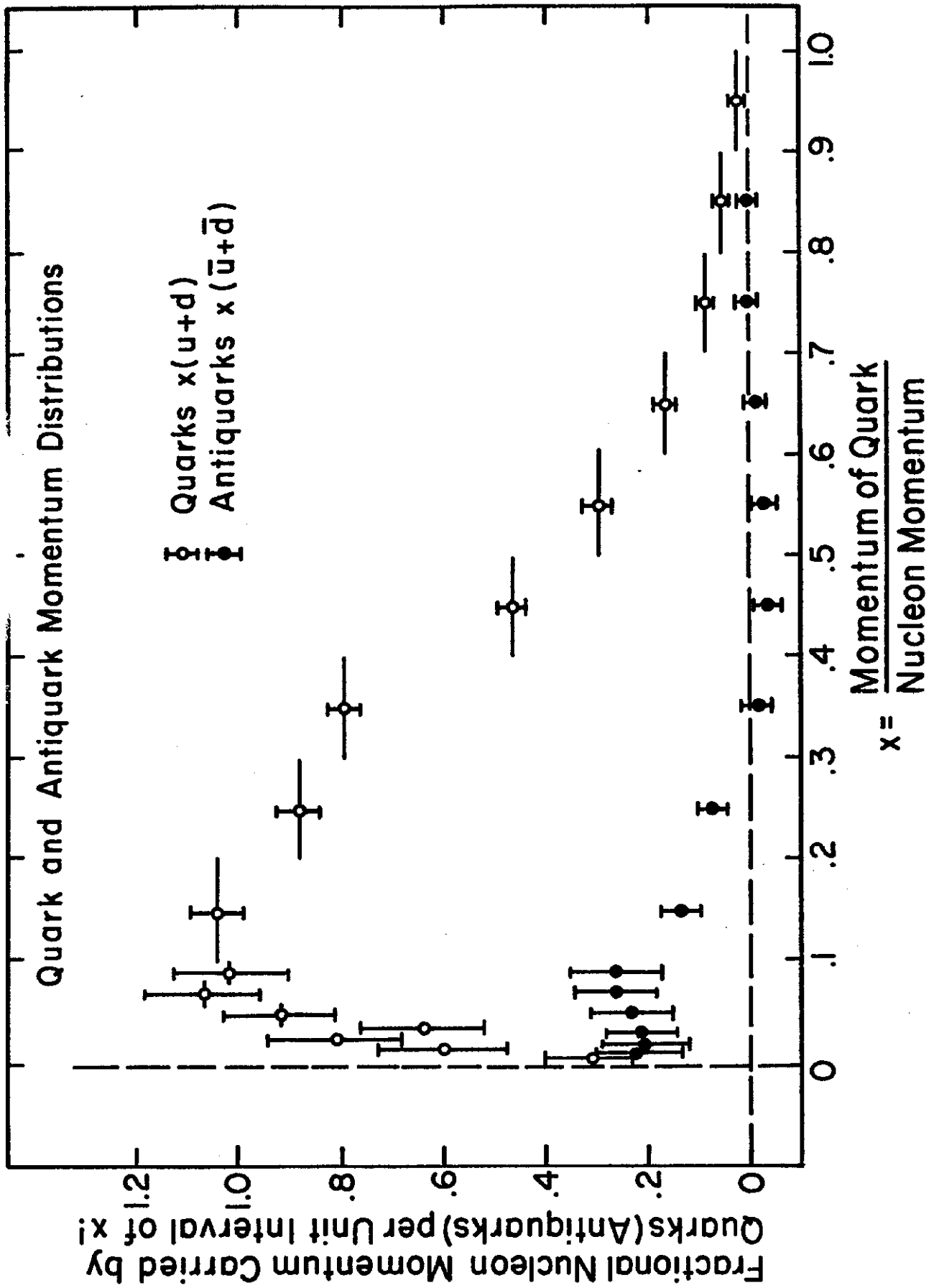


Figure 4

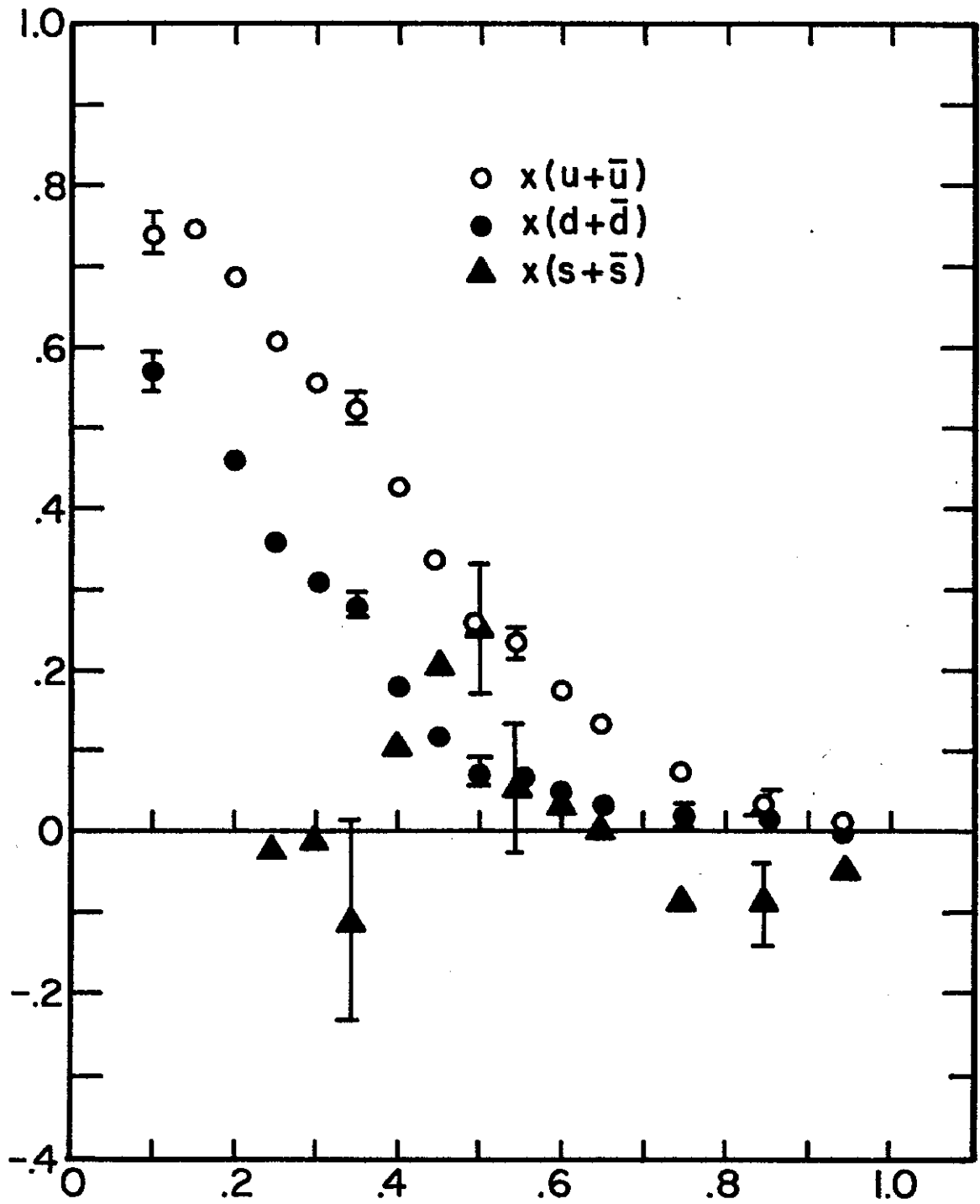


Figure 5

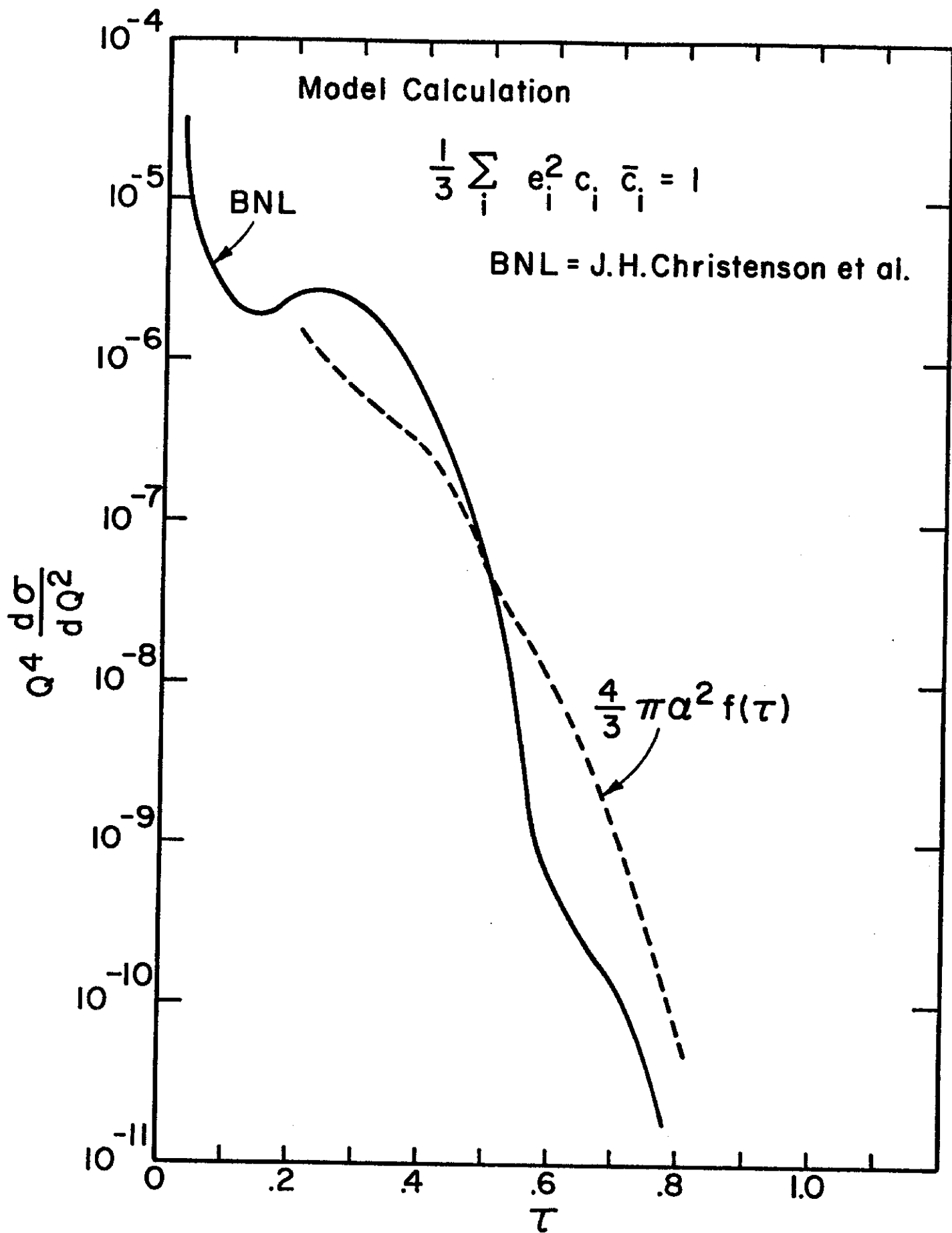


Figure 6

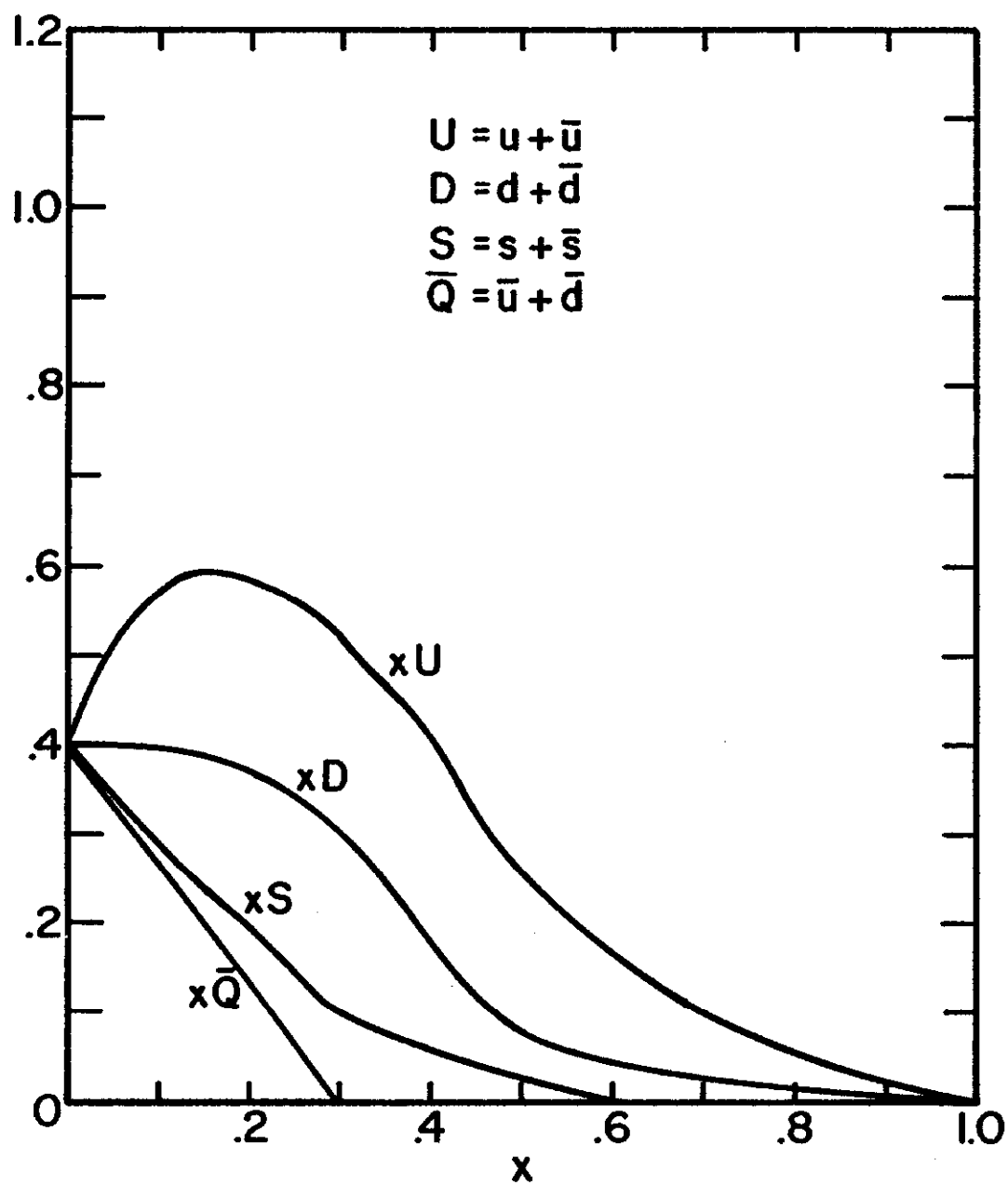


Figure 7

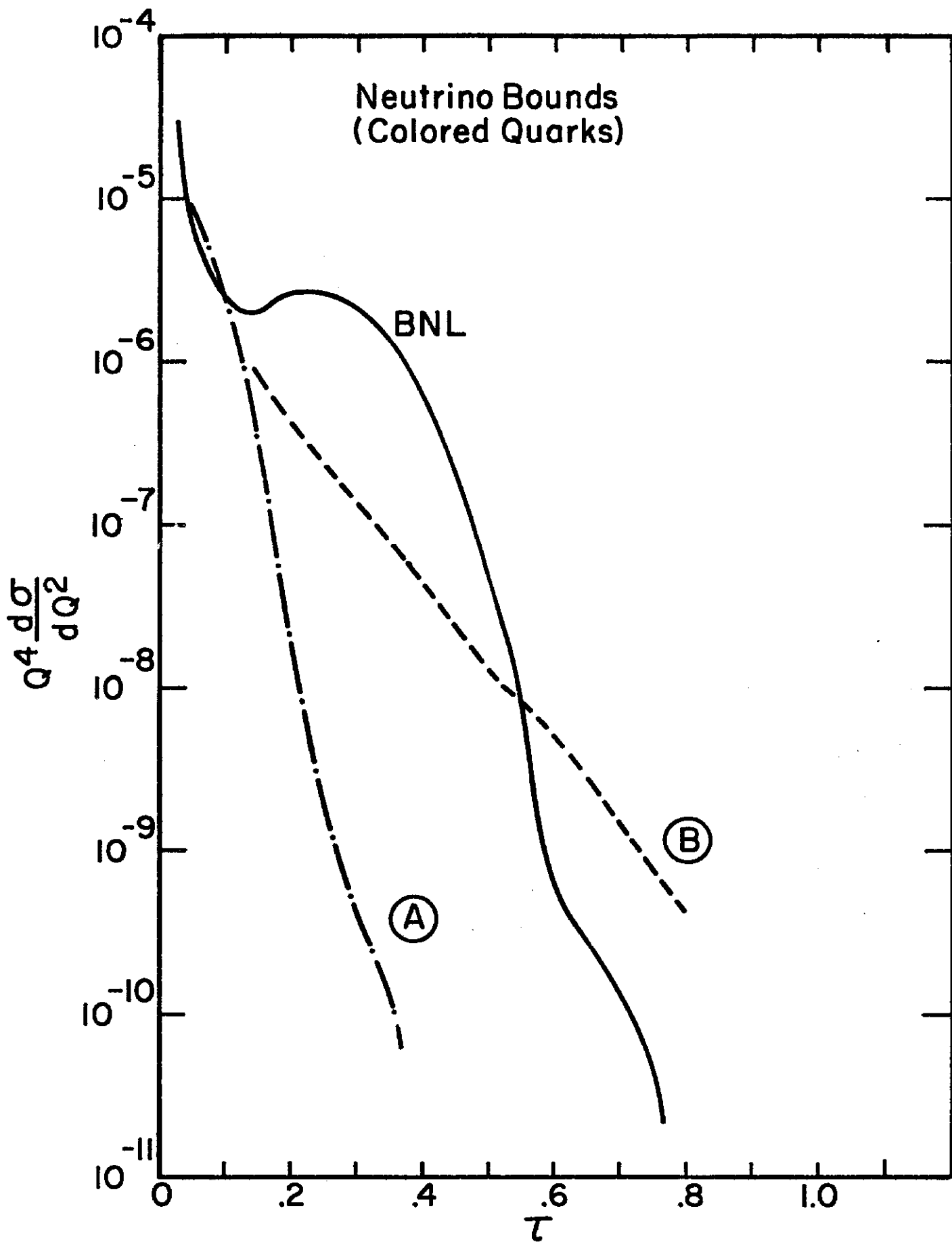


Figure 8